

Evaluation of Near-infrared Spectroscopy as a Rapid Method for Estimating the Carbon Stored per Unit Area in a Wetland



Final Report to the Manitoba Climate Change Action Fund on Project #15

December 2002

D.F. Malley¹, C. McClure¹, P.D. Martin¹, N. Firlotte¹, G. Goldsborough² and M. Sheppard³

¹PDK Projects, Inc.; ²University Field Station (Delta Marsh), University of Manitoba, Winnipeg MB;
³ECOMatters Inc., Suite 105, W.B. Lewis Business Centre, 24 Aberdeen Ave., Pinawa MB

PDK Projects, Inc.

365 Wildwood Park
Winnipeg MB R3T 0E7

#2 - 12 McGillivray Place
Winnipeg MB R3T 1N4

www.pdkprojects.com



Copyright ©PDK Projects, Inc. 2002

Executive Summary

The purpose of this study was to develop and evaluate a rapid, cost-effective method using near-infrared spectroscopy (NIRS) for estimating the quantity of total C per unit area (g cm^{-2}) in a lacustrine wetland. Three representative sites in Delta Marsh, on the shore of Lake Manitoba, Manitoba were sampled, Crescent Pond, a small isolated, sheltered, clear-water pond; Eaglenest, a larger bay unconnected to Lake Manitoba; and Cadham Bay, a large, deeper, turbid-water bay connected to the lake. Duplicate cores were collected at each site for a total of 6 cores. Cores ranged in length from 52 to 75 cm long and, at least in Cadham Bay, are believed to contain most of the carbon accumulated in the 2500 y geological history of the marsh. The 1-cm thick sections of the cores, comprising the samples in the study, were scanned with two NIR instruments with differing optical systems, data collection time, wavelength range, and field-portability, the Foss NIRSystems Inc. model 6500 visible/NIR scanning spectrophotometer and the Zeiss Corona spectrometer. Samples were scanned field-moist ("as is") and dry. Principal component analysis of the spectral data indicated qualitative differences in the samples among sites that are postulated to be due to variation in the influences of terrestriality vs limnology on the sites.

Calibrations were developed for moisture between the spectral data and gravimetric moisture determined in the samples and for C in the dried and field-moist samples. The NIR-predicted values for moisture agreed 93 and 94% with moisture determined by oven drying the samples for the 6500 and Corona instruments, respectively. These calibrations were judged using statistical criteria to be "excellent". The NIR-predicted values for C in the dried samples agreed 95 and 90% with the C values obtained by combustion for the 6500 and Corona instruments, respectively. For field-moist samples, the NIR-predicted values for C agreed 86 and 87% with the C contents calculated on a wet weight basis from the combustion reference data for the 6500 and Corona, respectively. These calibrations are judged to be "successful" to "excellent".

The total C contained in the six cores determined using the 6500 was 2.51, 2.79, 2.99, 2.49, 3.24, and 2.87 g cm^{-2} . Variability in core length affected the total C. Total C calculated for slices 2 to 51 cm, common to all cores, was 2.42, 2.43, and 2.06 g cm^{-2} for Crescent Pond, Eaglenest and Cadham Bay, respectively. Crescent Pond and Eaglenest were highly similar in C profiles; Cadham Bay contained lower C content above 50 cm. The results for C per unit area for each core were very similar between the 6500 and Corona NIR instruments. The coefficient of variability (deviation as a % of the mean) for total C between the two instruments for the six cores varied from 0.05 to 2.74 %.

Near-infrared spectroscopy is a feasible method for the determination of C inventories in wetlands when combined with effective sampling of the full depth of the organic C layer, appropriate sampling of spatial variability in the depth of the organic layer within representative habitats of the wetland, and measurement of areal extent of the representative habitats. It is expected from the literature that the technique can be utilized in peatlands as well as in lacustrine wetlands. Field-portability such as available in the Zeiss Corona can further reduce cost, time and effort, and increase efficiency.

Acknowledgments

This study was funded by Manitoba Climate Change Action Fund of the Government of Manitoba.

Assistance with field sampling at Delta Marsh was provided by Dr. Dale Wrubleski, Research Scientist, Ducks Unlimited Canada Institute for Wetland and Waterfowl Research, Stonewall MB, and Pascal Badiou, PhD Student, Department of Botany, University of Manitoba, Winnipeg MB.

We gratefully acknowledge the in-kind support of Foss NIRSystems Inc., Silver Spring MD with instrumentation, software, supplies, and technical support.

Carl Zeiss, Germany, and Product Manager, Michael Rode, are acknowledged for the generous loan of the Corona® VIS NIR instrument with software, supplies, and technical support.

ECOMatters Inc., Pinawa MB assisted by providing laboratory equipment on loan. Barbara Sanipelli assisted with the equipment transfer and provided technical assistance.

Brian Hauser, Freshwater Institute, Department of Fisheries and Oceans, provided a description of some methods.

The cover photo and other aerial photos in the text are courtesy of the University of Manitoba Delta Marsh Field Station.



Table of Contents

Executive Summary.....	2
Acknowledgments.....	3
Introduction.....	5
Near-infrared Spectroscopy.....	5
Purpose.....	6
Methods.....	6
Sampling Location.....	6
Formation and History of Delta Marsh.....	9
Field Sampling.....	10
Sample Processing.....	12
Chemical Analysis.....	15
Near-infrared Spectroscopy using the Foss NIRSystems Model 6500.....	15
Near-infrared Spectroscopy using the Zeiss Corona® 45 VIS NIR Spectrometer.....	18
Statistical Analysis and Calibration.....	19
Principal Component Analysis.....	19
Calibration Procedure Using The Unscrambler®.....	19
Statistical Evaluation of Calibrations.....	20
Calculation of Carbon per Unit Area from Cores.....	21
Results.....	22
Chemical Composition.....	22
Spectral Data.....	25
Principal Component Analysis of Spectral Data.....	27
NIR Prediction of Moisture and Carbon in Cores.....	34
Estimation of Carbon per Unit Area.....	39
Discussion.....	41
Effectiveness of Sampling.....	41
Qualitative Differences Among and Within Cores.....	41
Quantitative Analysis of Moisture and Carbon Samples.....	42
The Potential for Near-infrared Spectroscopy for On-site Determination of Carbon in Wetlands and Peatlands.....	43
References.....	44
Appendix I. NIR-predicted C content in each slice of each of the six cores in this study.....	46

Introduction

Wetlands cover approximately 14% of Canada's land surface (Statistics Canada 2000) and contain over 150 Gt of carbon, i.e., about 60% of Canada's carbon stock. Canada contains 24% of the world's wetlands (Statistics Canada 2000). The areal coverage by wetlands among the provinces is the greatest in Manitoba where wetlands cover 224,700 km² (Statistics Canada 2000) or 41% of Manitoba's 548,495 km² of land area.

Wetlands have the highest density of carbon of all land-based ecosystems. Wetlands absorb and emit carbon but generally absorb more carbon than is given off. Wetlands can be a source of the greenhouse gas, methane. This phenomenon is difficult to quantify on a landscape scale. While there may be a variety of opportunities to enhance wetlands and sequester carbon, there are few baseline data to know the conditions under which natural wetlands are net sinks or sources for greenhouse gases. This paucity of data makes it difficult to verify and quantify activities intended to cause wetlands to sequester carbon.

In 1992, the world's nations resolved to take action about the prospect of global climate change by formulating the United Nations Framework Convention on Climate Change (UNFCCC). Since then, the Conference of Parties (COP) of the UNFCCC, the countries that were signatories to the convention, have been meeting to develop the mechanism by which the nations of the world would bring about the UNFCCC. COP3 in Kyoto established greenhouse gas emission targets by the industrialized nations. At COP6 in The Hague, there was considerable controversy over the role of carbon sinks in reaching emissions targets. Included in the controversial aspects of carbon sinks were 1.) the permanence vs reversibility of the carbon stored, 2.) the difficulty of measurement of inventories of carbon stored and verification of actions that change inventories; 3.) the role of natural vs intentional human activity in changing inventories, and 4.) the extent to which various countries have access to carbon sinks.

If wetlands are to be utilized in a national plan of net carbon emissions reduction, methods need to be developed to inventory the carbon in them, monitor and verify changes in inventory, and monitor the functioning of wetlands with respect to net exchanges of carbon dioxide and methane. There are at present no practical methods for estimating the carbon inventory of a wetland and virtually no feasible method for estimating carbon quality on a landscape scale that indicates whether the carbon is permanent or transitory. A method used world-wide in commercial applications and in environmental R&D for the quantification and analysis of organic matter, near-infrared spectroscopy, is a good candidate for the cost-effective determination of carbon in wetland soil.

Near-infrared Spectroscopy

Near-infrared spectroscopy (NIRS) is a 30-year old technology used primarily for the rapid determination of organic constituents in foods, feed, pharmaceuticals, petrochemicals and other commodities (Williams and Norris 2001). Near-infrared radiation (780 to 2500 nm) is absorbed by covalent bonds in intact samples between atoms of C, H, O, N, and S. Spectral data from a set of samples are correlated with chemical analytical or functional data on the same samples.

These statistical correlations, called calibrations, are entered into the NIR instrument's computer and are used to predict the parameters of interest in unknown samples within 2 minutes or less.

NIRS has been reported by a number of authors to accurately determine total C, organic C, and moisture in soils (Dalal and Henry 1986; Morra et al. 1991; Confalonieri et al. 2001; Ludwig and Khanna 2001; McCarty and Reeves 2001; Ben-Dor 2002; Martin et al. 2002) and sediment (Malley et al., 1999; Malley et al. 2000).

NIRS has been shown to be effective not only in quantitative determination of C, but also in the analysis of C quality. It has been used to determine fractions of C of differing quality during the decomposition of organic material (McLellan et al. 1991a,b; Joffre et al. 1992; Gillon et al. 1993; Ben-Dor et al. 1997).

In addition to determining constituents in soil, NIRS has been used to predict functional properties of samples based on their organic composition. With NIR spectroscopical analysis of forest humus, 75 to 82% of the variances in microbial biomass determined by chloroform fumigation-extraction, metabolically active proportion of the microbial biomass, and fungal biomass as humus ergosterol content were explained (Pietikainen and Fritze 1995). NIRS has been used to model microbial basal respiration rate during aerobic decomposition of organic matter in forest soils where NIR explained 92 to 98% of the respiration rate (Nilsson et al. 1993).

Purpose

This project is intended as an initial phase of a larger project planned at applying near-infrared spectroscopy as one analytical tool to facilitate:

- a. estimating the total amount of C stored (inventory) in wetlands/peatlands
- b. estimating quantities of C of various composition
- c. estimating the exchange of CO₂ and methane between peatlands and the atmosphere.

The specific purpose of this feasibility study was to develop and evaluate a rapid, cost-effective method using near-infrared spectroscopy for estimating the quantity of total C (g cm⁻²) in a wetland. A lacustrine wetland was selected as the sampling location because of its accessibility and prior knowledge of the site. This report describes the results from the prediction of C and moisture in 1-cm thick sections from cores from three representative areas of Delta Marsh, Manitoba. A total of 6 cores was analyzed. Samples were scanned on two NIR instruments, a bench-top spectrophotometer and the field-portable Zeiss Corona spectrometer.

Methods

Sampling Location

Sampling was performed at Delta Marsh on the south shore of Lake Manitoba near the Delta Marsh Field Station, a field research and teaching facility of the Faculty of Science at the University of Manitoba at 98E 23'W, 50E 11'N. Delta Marsh is a "Wetland of International Significance" under the Ramsar Convention (The Bureau of the Convention on Wetlands, 2002),

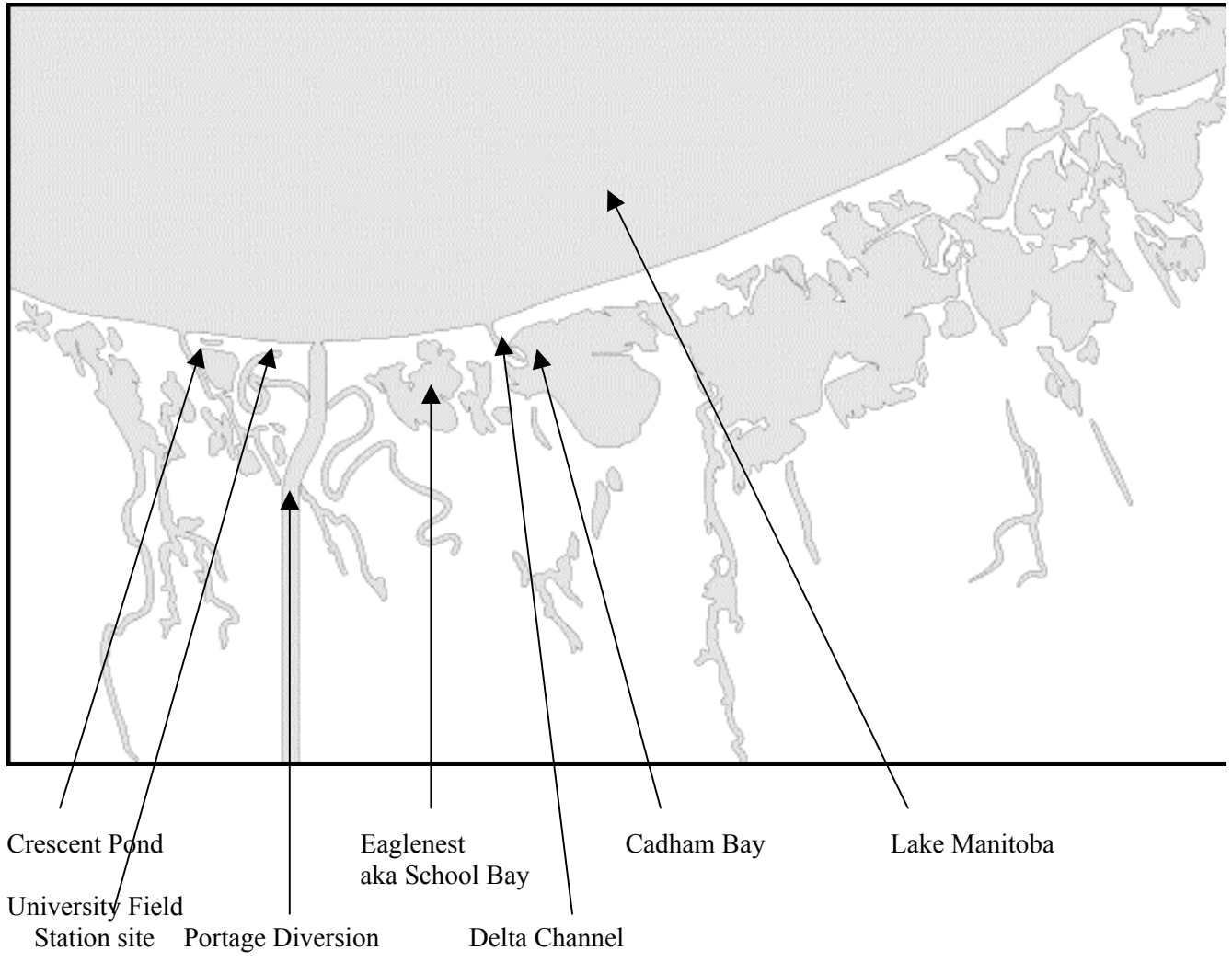


Fig. 1. Map of the bays and channels of Delta Marsh on the south shore of Lake Manitoba showing the location of the University of Manitoba Field Station and the three sampling sites, Crescent Pond, Eaglenest, and Cadham Bay. Map is from http://www.umanitoba.ca/delta_marsh/

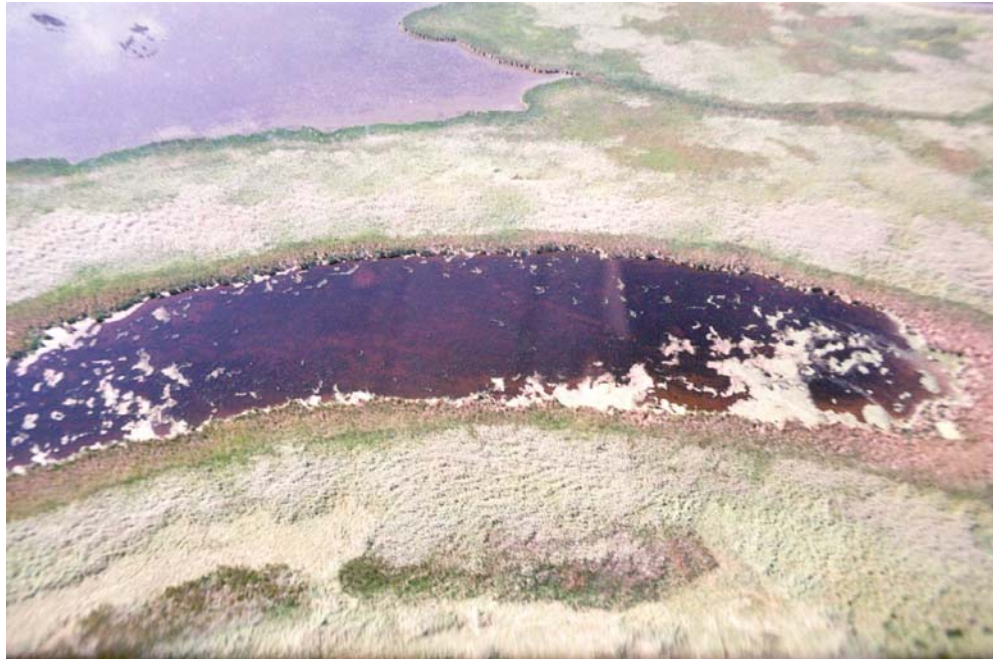


Fig. 2. Crescent Pond, a small isolated, sheltered pond



Fig. 3. Eaglenest, aka School Pond, a large isolated pond. Lake Manitoba is in the foreground



Fig. 4. Cadham Bay connected to Lake Manitoba through Delta Channel (outside of photo). Lake Manitoba is at the upper far left. The road in the foreground is the Delta Road to the Field Station.

and one of the largest lacustrine marshes in North America. It is the one of two Ramsar-listed marshes in Manitoba. It is currently estimated as 18,500 ha in area and 2,500 years old (Sproule 1972).

Formation and History of Delta Marsh

The formation of the marsh began about 4,500 y ago (Teller and Last, 1981). At that time, the Assiniboine River flowed into the south-western end of Lake Manitoba. The river produced a sandy delta that expanded into the lake. Easterly currents redistributed sand so that by 2,500 y ago the barrier beach had cut off the wetland now referred to as Delta Marsh.

As described by Shay (undated), the marsh has low relief with an elevation of only 4.4 m from the bottom of the deepest bay to the highest point on the ridge. Water depth throughout much of the marsh is only 1 m. The water is nutrient-rich and supports a luxuriant growth of algae, submerged aquatic plants, and emergent vegetation such as bulrushes, cattails and the giant reed, *Phragmites*. The productivity of marsh species is estimated at more than $1,000 \text{ g m}^{-2} \text{ y}^{-1}$. Although one might expect the marsh to have rapidly filled in as a result of this high productivity, this hasn't happened. Marsh vegetation patterns have been stable for more than 2,000 y as shown by paleolimnological analysis of two cores from Cadham Bay (Sproule 1972). The pollen assemblages, and the species of submerged aquatics, cattails, sedges, and damp ground annuals are the same as those present today. There were changes in the amount of pollen correlated with cycles of lake water level

fluctuations. Since 1924, Lake Manitoba water levels fluctuated with a cycle on the order of a decade. According to Shay (undated), these fluctuations are responsible for the lack of filling-in of shallow Delta Marsh. With the building of the Fairford dam in 1961, the lake level has been regulated with a target level of 247.5 m height and the marsh is considered to be in danger of filling in and being lost as a wetland.

The two cores taken by Sproule (1972) from Cadham Bay appear to be the only ones collected from the marsh available to indicate the depth of organic matter accumulation over the life of the marsh. Sproule (1972) collected his cores 80 and 150 m from the northern shore through the ice in 1 m water depth using a Livingstone-Vallentyne piston sampler with a diameter of 3.8 cm. Penetration was limited due to increasing compaction of the heavy clay sediment. These cores were 219 and 385 cm long. Fossils associated with marsh vegetation extended down to about 100 cm. The depth of 102-106 cm in one core was radiocarbon dated at $2,400 \pm 230$ y before present. In other words, the 2,400 y history of the marsh in the part of Cadham Bay sampled by Sproule is represented in a core 100 cm long.

Field Sampling

Three sites in Delta Marsh (Fig. 1) were sampled. These sites were selected as representative of several aquatic portions of the marsh differing in degree of influence of the aquatic ecosystem. These sites were Crescent Pond, a small isolated, clear-water pond, close to the beach ridge and sheltered (Fig. 2); Eaglenest, also known as School Bay, a larger bay unconnected to the lake (Fig. 3); and Cadham Bay, a large, deeper, turbid-water bay connected to Lake Manitoba through Delta Channel (Fig. 4). The sampling point in Cadham Bay was chosen as close as possible to the vicinity of the sites sampled by Sproule (1972).

Sampling was performed on 6 April 2002 by drilling holes through the ice with an ice auger. Water depth, not including the depth of the ice, varied from about 10 cm in Crescent Pond, to about 0.5 m in Eaglenest, to about 1 m in Cadham Bay. Core tubes of PVC, 7.5 cm i.d., about 3 m in length were inserted into the sediment as deeply as possible by hand (Fig. 5). The core tubes were withdrawn, holes were drilled in the sides above the top of the core to allow water to escape, and the tubes were sawn off at the top of the sediment so that sediment completely filled the core tubes (Fig. 6). Both ends were capped and sealed with duct tape (Fig. 7). Duplicate cores at each site were taken within a few m of each other for a total of six cores. Cores varied in length from 52 to 75 cm.

Cores were transported to the PDK Projects, Inc. laboratory in Winnipeg on 7 April 2002 and stored at 4° C until sectioned.

Table 1. Locations of coring and lengths of duplicate cores

Location	Type of Site	Co-ordinates ¹ of Sampling Sites	Length of Cores, cm
Crescent Pond	small, clear, isolated pond	5,559,284 meters northing, 542,506 meters easting	A = 53; B = 58
Eaglenest Bay, aka School Bay	large bay unconnected to the lake	5,558,224 meters northing, 547,423 meters easting	C = 63; D = 52
Cadham Bay	large, turbid bay connected to the lake	5,559,475 meters northing, 549,995 meters easting	E = 75; F = 71

¹UTM coordinates, zone 14.

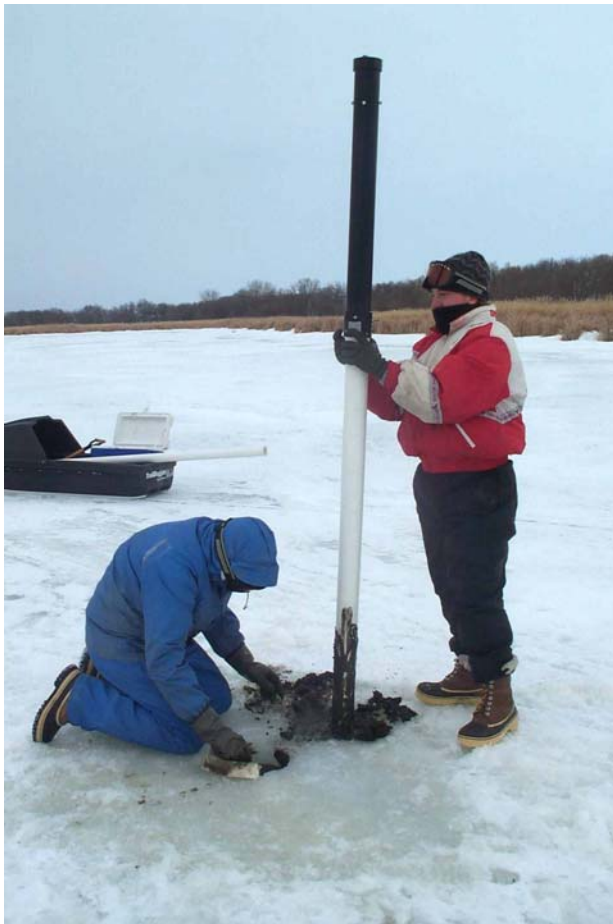


Fig. 5. Core tube being withdrawn from the water column following collection of the sediment core



Fig. 6. Core tube sawn off at the top of the sediment ready to be capped for transport



Fig. 7. Core tube before sectioning

Sample Processing

Core tubes were sectioned by cutting across the diameter of the caps using a circular saw fitted with a masonry (abrasive) blade (Fig. 8). A carbide tip rip tooth blade was used for the initial core, but it resulted in slivers of PVC being present in the core material. The tubes were then placed in a custom-built holder that held the tubes securely during sawing (Fig. 9) and contained a guide for the saw. The holder exposed the tube along its length and the tubes were cut to match the cuts in the end caps. The first cut side of the tube was sealed with duct tape before the second side was cut (Fig. 10). When both sides were cut, the tape was removed and a knife drawn lengthwise along the cuts to divide the cores into two halves longitudinally. The two halves of the core were separated from one another (Fig. 11). The material was generally consolidated, except for the first one or two cm that tended to be a thick slurry.

One half of each core was sectioned into 1-cm thick sections using a plastic knife. The sections (i.e., samples) were placed in 18 oz Whirlpak bags. Each bag was weighed before and after filling to obtain a wet weight of each sample. Portions were removed for scanning in the field-moist state and returned to the bag. Each sample was then divided into two portions, each placed in an aluminum weigh pan (Fig. 12). The pans were weighed before filling and periodically during drying of the samples at 110° C to ensure drying to constant weight, requiring 24 to 48 h. The dried material was solid, light to medium grey in colour (Fig. 12). All samples were pulverized with a mortar and pestle and stored in borosilicate glass scintillation vials until they were scanned (Fig. 13).



Fig. 8. The ends of the core tubes were sawn with a circular saw. The opening was sealed with duct tape.



Fig. 9. Core tubes were opened lengthwise by circular saw. A custom-made holder held the tube firmly and served as a guide for the saw so that the blade moved along the tube at the correct position.



Fig. 10. The first lengthwise cut on the core tube was taped with duct tape to prevent loss of material while the second cut was made on the opposite side of the tube



Fig. 11. The core in one half of the core tube completely filled the length of the tube. The material was generally consolidated, except for the first one of two cm at the top that were a thick slurry.



Fig. 12. After scanning on the NIR instruments each slice was divided into two portions and oven-dried to constant weight



Fig. 13. The dried samples were pulverized using a mortar and pestle and placed in glass scintillation vials for scanning in the dry state and subsequent chemical analysis

Chemical Analysis

Dried, ground samples of the wetland soil were analyzed for C by the Dumas combustion method using a Exeter Analytical CE440 Elemental Analyzer. Quantities of 2-12 mg of soil were combusted in an oxygen-helium atmosphere at 980 °C. Helium carrier gas was used to sweep the combustion products over a heated bed that oxidized the combustion gases to CO₂, H₂O, and oxides of N while removing interfering halogens, S, and P. The gas stream passed over hot Cu at 700 °C where oxides of N were reduced to N₂ and excess O₂ was removed. After mixing, the gases sequentially passed through high precision thermal conductivity detectors and gas traps that sequentially removed H₂O and CO₂. The remaining gas, N₂, was measured against the pure helium carrier gas. Concentrations of C in samples were expressed on a dry weight (d.w.) basis. Carbon concentrations on a wet weight (w.w.) basis were obtained from the calculation:

$$[C] \text{ w.w.} = \frac{100 - \% \text{ moisture}}{100} \times [C] \text{ d.w.} \quad (1)$$

Near-infrared Spectroscopy using the Foss NIRSystems Model 6500

NIR spectra were recorded using a Foss NIRSystems Inc (Silver Spring MD) Model 6500 visible/NIR scanning spectrophotometer in the reflectance mode. Light from the light source, reflected from the sample as diffuse reflectance, is recorded by the detector. In the reflectance mode, the light source and the detector are on the same side of the sample cell. The instrument was operated using Vision® software. This monochromator instrument records 32 scans from the sample over 50 sec and averages these as the sample scan. Before each day's operation, a diagnostic test was run to ensure that electronic noise and wavelength accuracy were within specifications.

For the field-moist samples, the 6500 was used with the standard sample transport (Fig. 14). In this configuration, absorbance, i.e., $\log 1/R$ where R is reflectance was recorded every 2 nm from 400 to 2500 nm. Two detectors operate over this range, a silicon detector from 400 to 1100 nm, and a PbS detector from 1100 to 2500 nm. Field-moist, "as is", soil samples were placed in a standard 7.4 cm o.d. Foss sample cell (Fig. 15). This is a reflectance cell with quartz glass on one side of the cell and a solid surface on the other. The cell was placed in the upper module of the instrument for scanning (Fig. 16). Between each sample scan, an internal reference ceramic was scanned and the reference spectrum was automatically subtracted from each sample scan. Triplicate scans were recorded on each sample, with the cell being turned 120° between scans. A sample scan plus the reference scan takes < 2 min.



Fig. 14. Foss NIRSystems model 6500 scanning spectrophotometer fitted with standard transport. The sample cell in Fig. 15 fits into a holder in upper part of the sample transport. The cell moves to the lower part of the sample transport for scanning.



Fig. 15. The standard sample cell, 7.4 cm o.d. used to scan the field-moist samples in the 6500 and Corona NIR instruments. The quartz window is 5.0 cm in diameter. The cell is shown here filled with a field-moist sample.



Fig. 16. The sample holder in the upper module of the 6500 with a sample cell in place



Fig. 17. The 6500 instrument (back) is turned on its side and connected to the Rapid Content Sampler (front) that is closed.



Fig. 18. The Rapid Content Sampler is open showing a dry sample in a scintillation vial in place for scanning through the quartz window (right). A mechanical iris is used to position the vial in the centre of the window. The external ceramic reference is in the centre of the photo

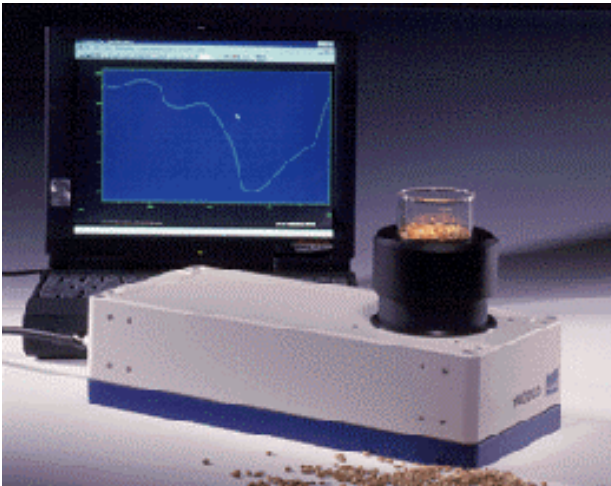


Fig. 19. Manufacturer's photo of the Zeiss Corona showing the black sensor head.



Fig. 20. The Zeiss Corona scanning the white reference inside a Foss standard sample cell. The reference was scanned between each sample. The samples were presented in the standard sample cell as in Fig. 15.

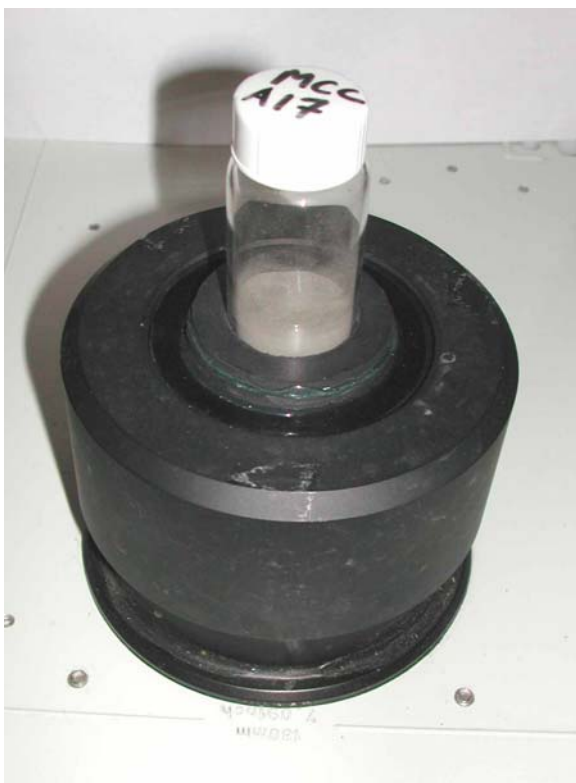


Fig. 21. Scintillation vial containing a dry sample in place on the Corona sensor head



Fig. 22. External ceramic reference in place on the Corona sensor head

The dried and pulverized samples in borosilicate glass scintillation vials were scanned with the 6500 configured with the Rapid Content Sampler (RCS) (Fig. 17). The RCS contains only the PbS detector and scans from 1100 to 2500 nm at 2 nm intervals. The RCS is designed for scanning through the bottom of pharmaceutical vials (Fig. 18). Between each sample scan, an external ceramic disc was scanned as the reference and the reference scan was automatically subtracted from each sample scan. The vial was shaken before each scan to present a different "view" of the sample to the instrument. Advantages of scanning dry samples in vials rather than in the sample cell are that fine particles are not lost in filling and emptying the sample cell, the moisture level in dry samples is stable, and handling each sample is faster.

Near-infrared Spectroscopy using the Zeiss Corona® 45 VIS NIR Spectrometer

The Zeiss Corona® 45 VISNIR 1.7 Spectrometer (Fig. 19) consists of a spectral measuring body, bonded with a concave grating that corrects aberrations, a fibre cross-section converter as an optical input and a diode array detector. It is compact, permanently aligned, robust, thermally stable, small, and possesses a high degree of light sensitivity.

The Corona 45 VIS NIR was operated using Aspect Plus software provided with the instrument. This recorded spectra as absorbance from 360 to 1700 nm at approximately 6 nm intervals. Two overlapping detectors operate over this range. Spectra can be recorded from each detector

separately, or they can be recorded over the entire range. The cut-off between detectors can be set within limits. Aspect software saves each spectrum in a separate file.

The field-moist samples in the Foss standard sample cell were placed on the upward-facing sensor head shown in Fig. 19 and the spectra recorded from 360 to 1700 nm. A ceramic reference provided by Zeiss was placed inside a duplicate cell and used as the system reference (Fig. 20). The cells were centered on top of a spacer ring mounted on the sensor head. Between each sample scan, the ceramic reference was scanned and the reference spectrum automatically subtracted from the sample spectrum. The sample cell was scanned a second time, to provide duplicate spectra for each sample.

In order to position the glass scintillation vials containing the dried, ground samples on the sensor head at the correct height, a sample holder was custom-designed and constructed. This fit on the ledge on the inside of the sensor head so that the bottom of the vial was at the correct height and the vial was centered (Fig. 21). Each vial was shaken and scanned twice. Between the scans, the external ceramic reference used with the RCS was scanned (Fig. 22) and the reference spectrum automatically subtracted from the spectrum of the samples. The holder for the external ceramic reference was also custom-designed and built.

Statistical Analysis and Calibration

Principal Component Analysis

Using multivariate analysis software, The Unscrambler® 7.6 (CAMO ASA Oslo, Norway), principal component analysis (PCA) was performed on the spectral data of the field-moist, "as is" samples and the dried samples from each of the two NIR instruments. Principal component analysis is a mathematical technique for resolving the variability in numerous wavelengths (700 to 1050) in a set of samples into a small number of underlying variables known as principal components or eigenvectors. The first principal component (PC1) accounts for the largest possible amount of variance in the data, and subsequent PCs account for successively less and less of the variance. Scores are the locations of individual samples along each PC. The scores can be plotted in two-dimensional x-y plots, or three-dimensional x-y-z plots. Normally PC1 is plotted against PC2, and PC1 may be plotted against PC3, or PC2 against PC3. Occasionally PC4 is also plotted. These plots provide information about patterns, groupings, similarities or differences among the samples. The closer samples are in the scores plot, the more similar they are with respect to each other in composition of spectrally-active components. Conversely, samples far away from each other are different from each other.

Calibration Procedure Using The Unscrambler®

The ability of NIRS to provide rapid analyses depends on the prior preparation of mathematical calibrations used to predict constituents, parameters or functionality in unknown samples. A calibration is a statistical correlation model relating the spectral data for a set of samples to the constituent data determined by conventional (reference) methods.

Calibrations were developed for moisture and C on field-moist samples, and for C on dry samples using scans from each of the two NIR instruments.

The first step in the calibration process for spectra obtained with the Foss NIRSystems model 6500 was inspection of all the spectra using Vision software. Where one of the triplicate spectra for the field-moist samples was different from the others, only two of the three were averaged. If the two spectra for the dry samples differed, the sample was rescanned. The spectra were examined for noise (fluctuations) at their ends. If noise is present, the wavelength range used for calibration can be reduced to remove the noisy areas.

Spectra recorded by the 6500 were exported as Near-infrared Spectral Analysis Software (NSAS) files from Vision software and imported directly into The Unscrambler. In Aspect, each spectrum was saved in a separate file and the wavelength interval between absorbance values was approximately 6 nm. In Aspect, spectral were files were bundled, and transformed through the "interpolation" function to 2 nm intervals. From Aspect, the spectra were exported as Grams 32 files and imported into The Unscrambler. In The Unscrambler, replicate spectra were averaged and the constituent data were added to the file containing the spectral data.

Calibrations were developed in The Unscrambler using principal component analysis/partial least squares regression (PCA/PLS). This regresses the PCs against the reference data for each constituent. Using the test set method, calibrations were developed on two-thirds of the samples and validated on the remaining third of the samples (every third sample was selected) using PLS1. PLS1 calibrates for one constituent at a time. Calibrations were developed and validated on untransformed spectral data and on the spectral data smoothed over 5, 11, 21, or 41 wavelength points (where wavelength points were at 2 nm intervals). Calibrations were also performed on data smoothed over each interval and then transformed to first or second derivative where the derivative interval, or gap, was 5, 11, 21, or 41 wavelength points. This gave a total of 37 trial calibrations. The calibration that resulted in the highest r^2 (coefficient of determination) between the NIR-predicted values in the validation set and the chemically-measured, reference values, and in the lowest Standard Error of Prediction (SEP) was selected as the best. The SEP is the standard deviation of the residuals about the 1:1 line between the reference values and the NIR-predicted values. Using the smoothing and derivative combination of this best calibration, calibration and validation were repeated twice more so that each sample was predicted in a validation set. In this way, all of the samples were predicted. NIR-predicted values for all of the samples from the validation sets were graphed as a function of the chemically-measured values. Also calculated was the ratio of the SD (standard deviation) of the reference values in the validation set to the SEP termed the RPD, and the ratio of the range of the reference values in the validation set to the SEP termed the RER. The regression statistics, r^2 , SEP, RPD, and RER were tabulated.

Statistical Evaluation of Calibrations

In the successful analysis of agricultural commodities, it is desirable that r^2 is > 0.95 , RPD is > 5 and RER is > 20 . Nevertheless, for samples of naturally-occurring materials such as soil and sediments that are more variable than commodities, several levels of performance are defined and used in this study. Excellent calibrations were those with $r^2 > 0.95$ and RPD > 4 . Successful calibrations have $r^2 = 0.9 - 0.95$ and RPD = 3 - 4. Moderately successful calibrations have $r^2 = 0.8 - 0.9$ and RPD = 2.25 - 3 and moderately useful ones have r^2 from 0.7 - 0.8 and RPD from 1.75 - 2.25. Calibrations with lower statistical performance may still be useful depending on the accuracy required in the field situation and whether or not better alternative field methods are available.

They are useful for screening purposes, such as for distinguishing among low, medium, and high values, or for selecting samples for costly conventional chemical analysis.

Calculation of Carbon per Unit Area from Cores

The sectioning of cores resulted in 372 duplicate samples. Of these 372, 192 were analyzed by combustion for C to provide the reference data for the C calibrations. Using the best calibration for C for each NIR instrument, [C] in each of the 372 field-moist samples was predicted. The amount of C in g cm^{-3} in each core slice was calculated:

$$C, \text{ g cm}^{-3} = \frac{(\text{NIR-predicted [C], mg g}^{-1} \text{ w.w.)} \times \text{wet weight of sample, g} \times 2}{1000 \times 44.179 \text{ cm}^2} \quad (2)$$

where each sample is half of a core slice and 44.179 cm^2 is the area of the complete slice. The quantity of C as g cm^{-3} was summed for each core to provide an estimate of C as g cm^{-2} .

Results

Chemical Composition

Overall, the samples from the six cores in this study varied in moisture content from 21.7 to 83.8 % (Table 2). The cores from the Crescent site had the highest mean moisture and the Cadham cores were lowest in mean moisture (Table 2). The moisture in all cores was highest at the surface and declined with core depth (Fig. 21). Moisture did not decline uniformly with depth but fluctuated down the cores. The duplicate cores from each site were similar but not identical in profile.

Table 2. Statistics for moisture and C determined by the reference methods in each of the six cores in this study

Parameter	Crescent #1 Core A	Crescent #2 Core B	Eaglenest #1 Core C	Eaglenest #2 Core D	Cadham #1 Core E	Cadham #2 Core F
No. of samples moisture, C	52, 30	58, 28	62, 37	51, 23	74, 37	71, 35
Mean \pm SD moisture, %	57.97 \pm 8.04	58.57 \pm 8.68	52.64 \pm 9.89	53.67 \pm 10.25	43.25 \pm 19.14	47.77 \pm 19.86
Range in moisture, %	43.87 - 75.22	40.80 - 83.78	35.42 - 70.74	41.62 - 72.73	21.66 - 76.16	23.48 - 77.21
Mean \pm SD C, mg/g d.w.	97.13 \pm 15.99	96.43 \pm 11.91	74.81 \pm 16.08	80.91 \pm 12.05	51.73 \pm 21.76	57.31 \pm 20.35
Range in C, mg/g d.w.	60 - 137	67 - 129	35 - 98	65 - 105	18 - 97	15 - 87

Fluctuations in moisture down the core reflect differences in intergrain porosity. Some levels in the core are more compacted than others. Compaction or high bulk density is associated with lower moisture levels. Changes in porosity or bulk density are affected by aspects of the depositional environment, such as different mineralogy or vegetation debris at the sediment-water interface as the deposition was occurring. Fig. 23 shows that the lowest water contents occurred at the bottom of the Cadham Bay cores. These moisture levels are typical of a silty sand.

Carbon concentrations, on a dry weight basis, over all the cores averaged 74.20 ± 24.52 mg g⁻¹ d.w.(range 15 - 137 mg g⁻¹). Carbon was highest in the cores from Crescent Pond, the site most isolated from Lake Manitoba, and lowest in Cadham Bay, most connected with Lake Manitoba (Table 2, Fig. 24).

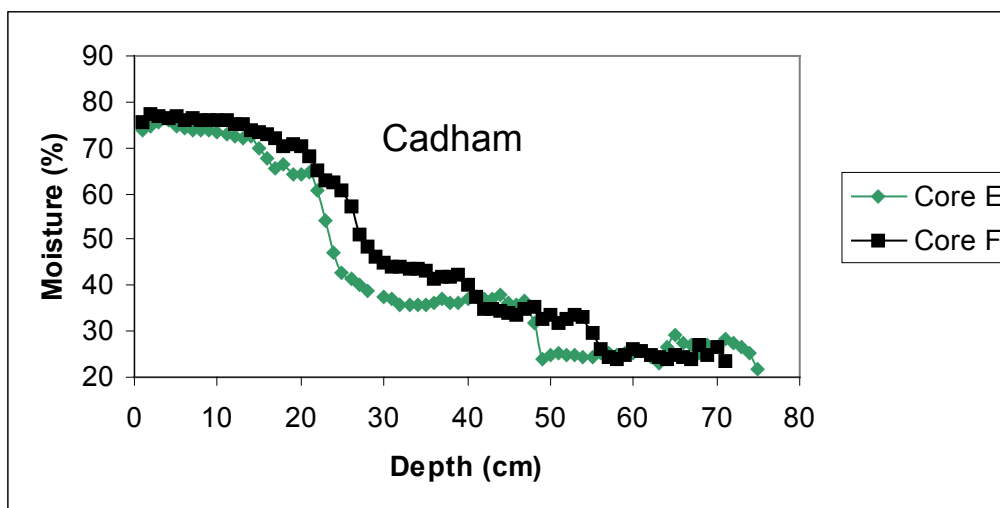
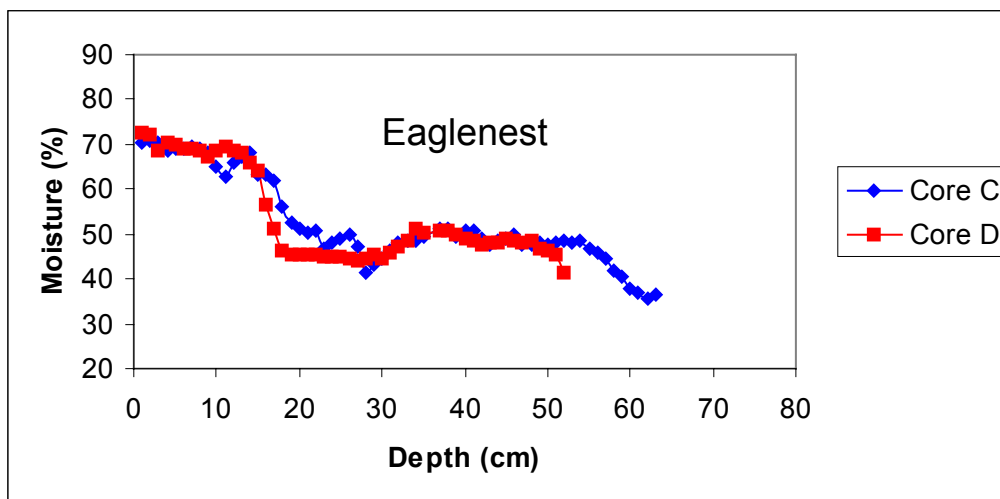
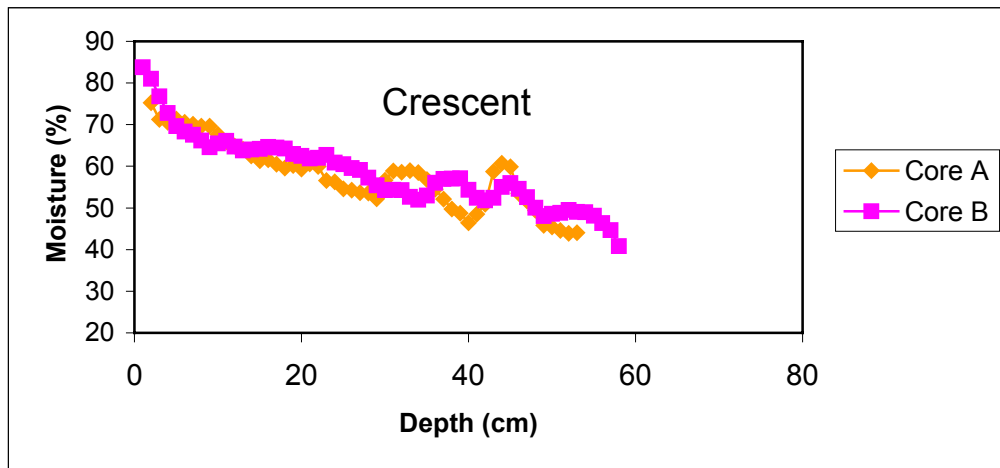


Fig. 23. Profiles for moisture determined by oven drying for the six cores in this study arranged in duplicates by site.

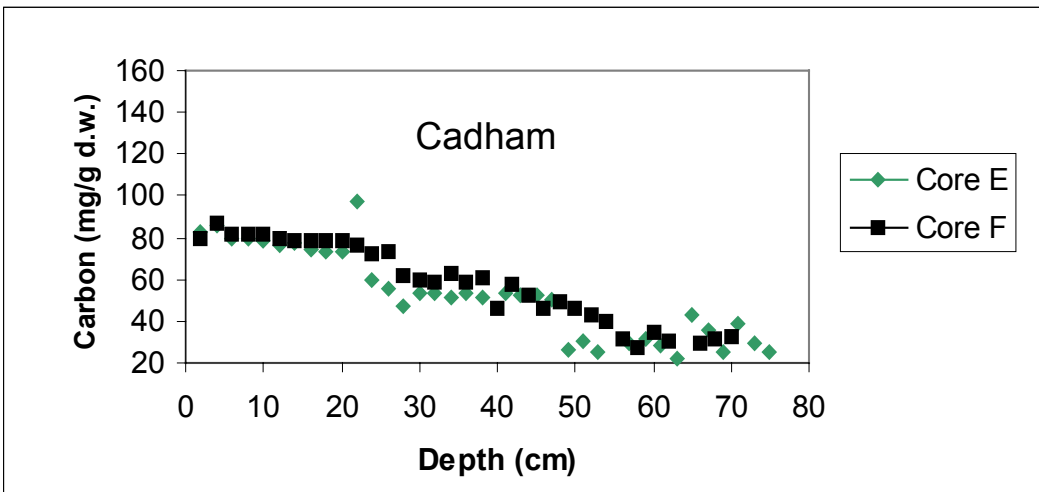
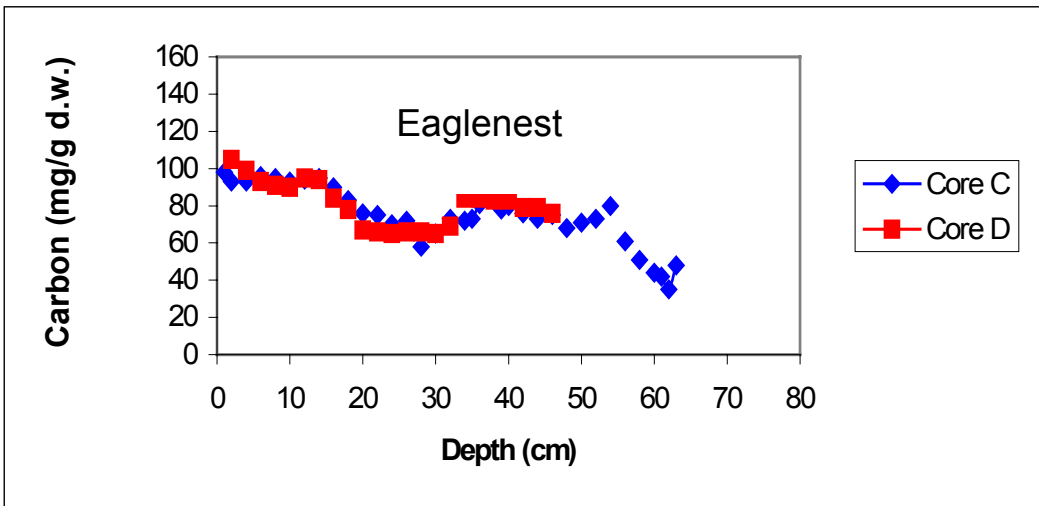
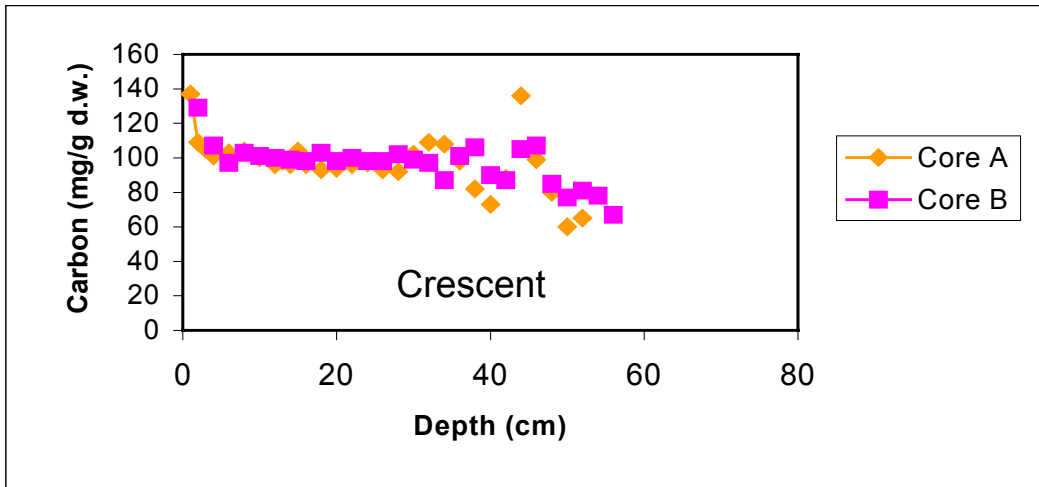


Fig. 24. Profiles for C, dry weight basis, determined by combustion for the six cores in this study arranged in duplicates by site.

Spectral Data

Representative spectra from field-moist, "as is", samples from Core A are shown in Fig. 25 for the 6500 and in Fig. 26 for the Corona. For both sets of spectra, the dominant features are absorbance bands of water, actually, the OH⁻ group in water. Three categories of water absorb in the NIR region, a) hydration water, incorporated into the lattice of minerals; b) hygroscopic water, adsorbed on soil surface areas as a thin layer; and c) free water, occupying soil pores (Ben-Dor 2002). The vibrations of the OH group produce absorbances at 950 nm (very weak), 1200 nm (weak), 1400 nm (strong) and 1900 (very strong) (Ben-Dor 2002). There is a weak band at 2200 nm as well. The spectra recorded by the 6500 are dominated by the bands at 1400 and 1900 nm (Fig. 25). Absorbance reaches values >1.8. Values below absorbances of 2.0 are useful for NIR calibration. Spectra recorded with the Corona show only the water band at 1400 nm (Fig. 26).

Spectra from dried and ground samples from Core A recorded with the 6500 show flatter spectra with lower absorbances (Fig. 27). Water bands at 1400 and 1900 nm are obvious, but now the band at 2200 nm is clearly seen.

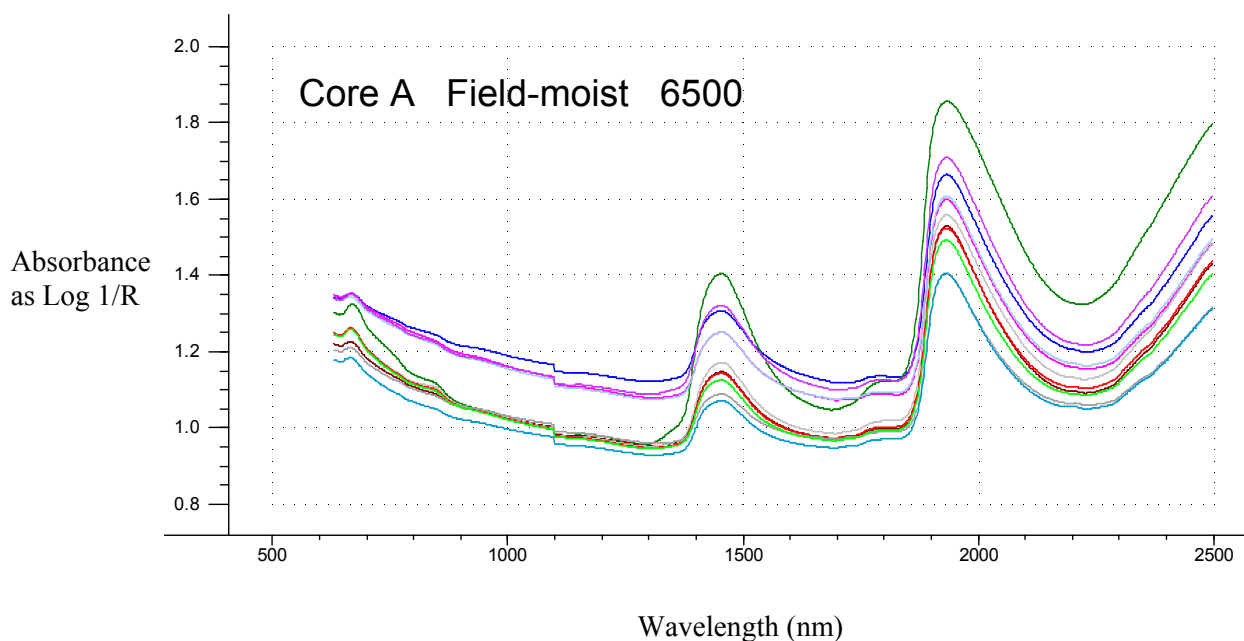


Fig. 25. Spectra from every 5th slice of Core A, Crescent Pond recorded with the 6500. Samples were field-moist, "as is". Wavelengths are from 630 to 2498 nm. The discontinuity at 1100 nm is caused by the change from one detector to another.

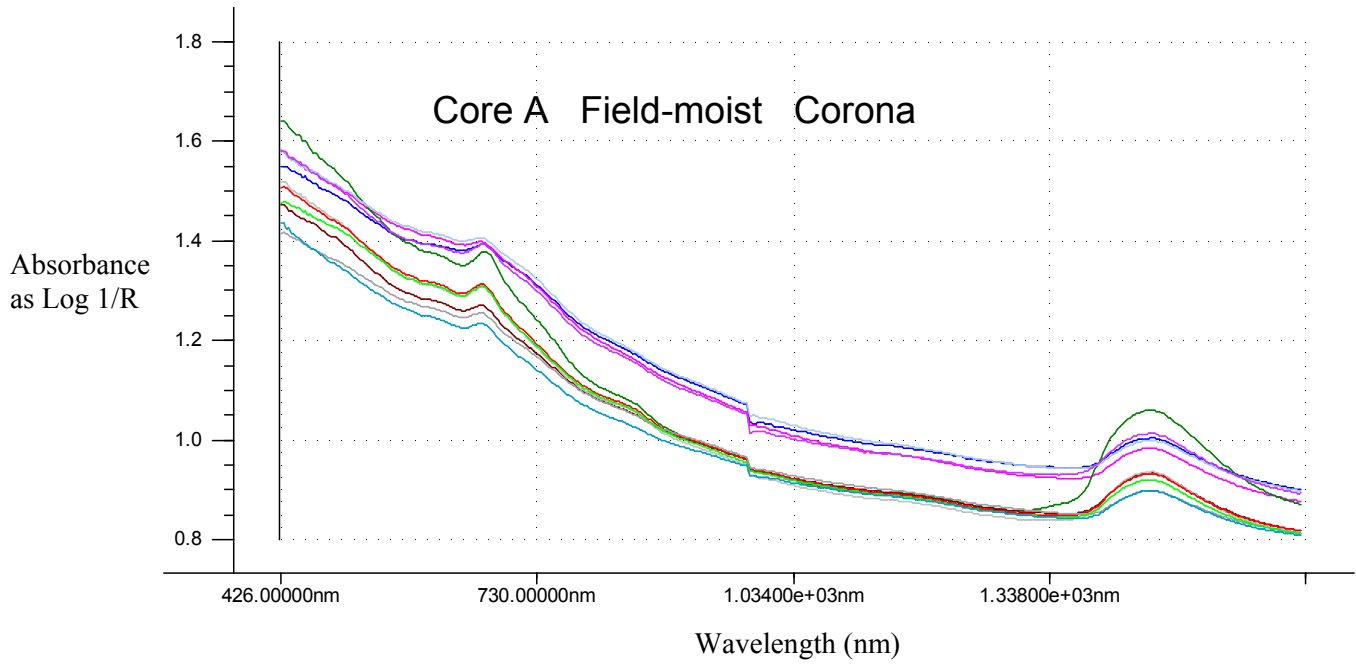


Fig. 26. Spectra from every 5th slice of Core A, Crescent Pond recorded with the Corona. Samples were field-moist, "as is". Wavelengths are from 426 to 1600 nm. The discontinuity at 980 nm is caused by a change from one detector to another.

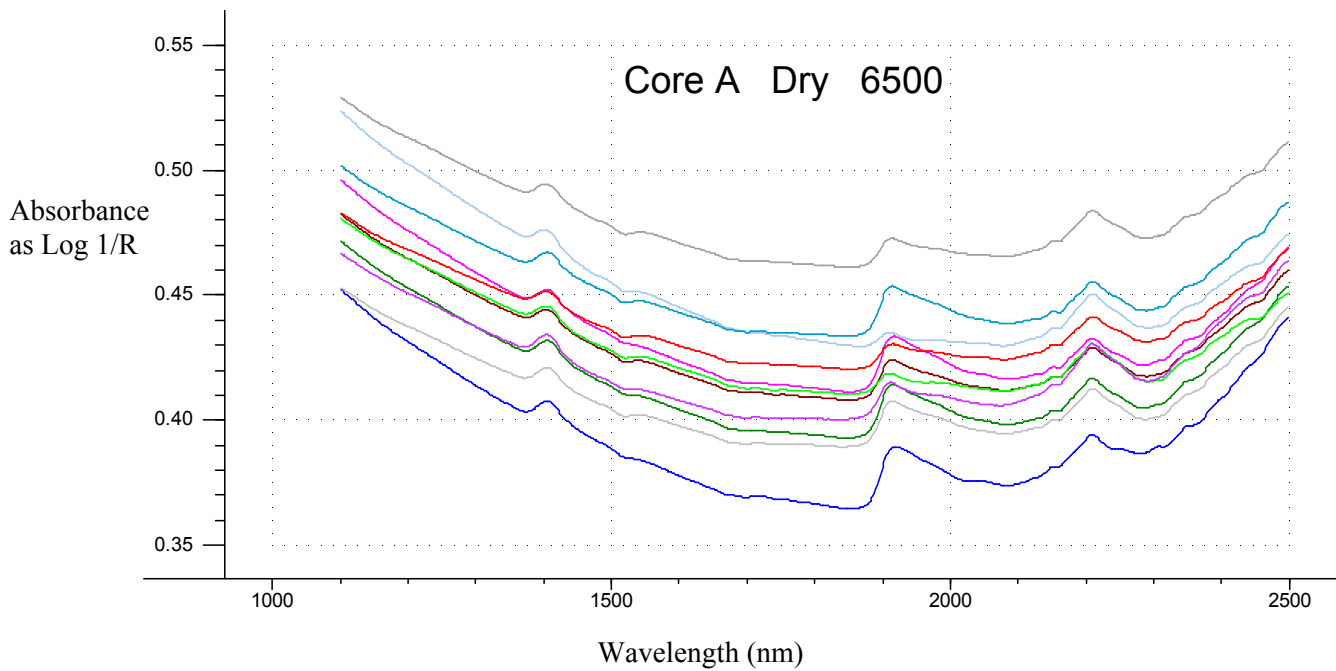


Fig. 27. Spectra from every 5th slice of Core A, Crescent Pond recorded with the 6500. Samples were dried and pulverized. Wavelengths are from 1100 to 2498 nm.

Principal Component Analysis of Spectral Data

Scores for the field-moist samples recorded with the 6500 are plotted against the first three principal components in Fig. 28 and 29. The first three PCs accounted for 77%, 13%, and 8% of the variability in the spectral data, respectively. Considering the scores of the samples on PC1 and PC2, the duplicate cores from each site were most similar to each other. There was complete separation of Crescent Pond cores from those at the other two sites whereas Eaglenest and Cadham Bay core samples overlapped somewhat (Fig. 28). The scores plotted on PC2 and PC3 gave the same results. Crescent Pond cores samples were completely separated from the other two sites and the samples from the latter overlapped somewhat (Fig. 29).

More detail on the scores for the spectra recorded with the 6500 for cores A, C, and E are shown in Fig. 30 to 32. In each case, the scores for the uppermost samples are in the left-hand side of the plot. The scores tend to move to the right of the plot and end up at the far right side. It is likely that moisture had an important influence on the scores. As Fig. 23 indicates, the uppermost samples in the core were the wettest and the lowest ones, the driest.

The PCA results for the spectra recorded using the Corona shown in Fig. 33 and 34 are similar to those of the 6500 in Fig. 27 and 28. Again, duplicate cores from each site generally overlapped each other, but C and D were more different from each other than they were when scanned with the 6500. The Crescent core samples were generally distinct from the other two sites, and Eaglenest and Cadham overlapped to some extent.

Scores for dry samples for spectra recorded with the 6500 are shown in Fig. 35 and 36. The first four PCs accounted for 67, 18, 6, and 2 %, respectively, of the variation in the spectral data. Compared with Fig. 28 and 29, samples from the duplicate cores from Crescent, A and B, tended to be more similar to each other, than did the samples from the duplicate cores from Eaglenest and Cadham. In cores, C, D, E, and F, there were samples that were similar to each other and to those from A and B, but there were other samples that were different from those in other cores. This was particularly the case for some samples from core C (Fig. 35, 36). Scores for cores A, C, and E are shown individually in Fig. 37 to 39.

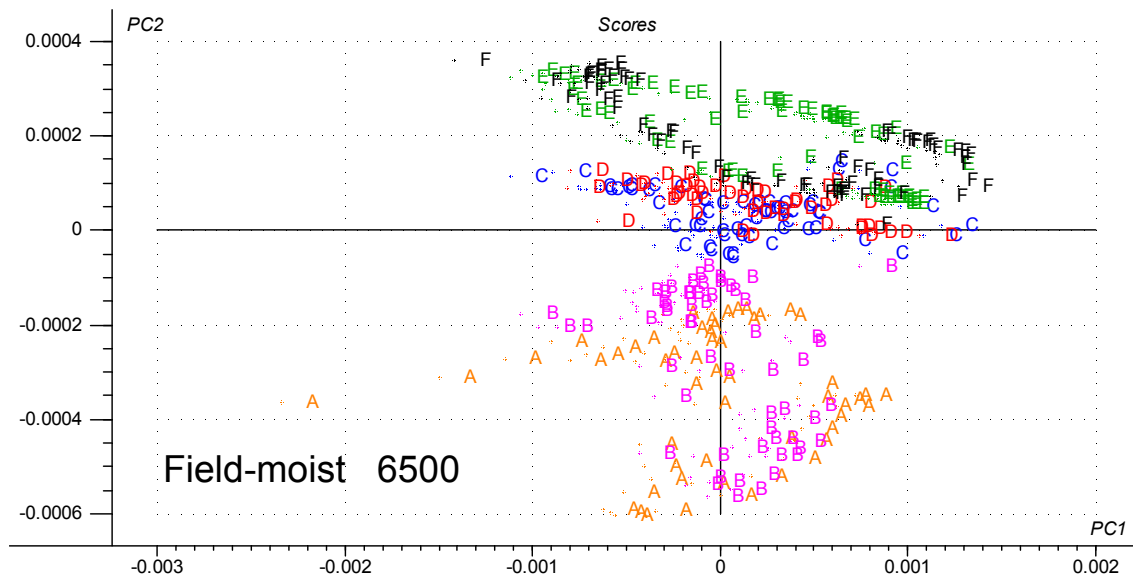


Fig. 28. Scores plot for the 371 samples from the six cores in this study on the first two principal components explaining the variability in the spectral data (600-2498 nm) recorded using the 6500. The spectra were recorded using the model 6500 spectrophotometer and the samples were in moist, "as is" state. The spectral were smoothed and transformed to the second derivative. The cores were A and B from small isolated Crescent Pond, C and D from Eaglenest unconnected to the lake, and E and F from Cadham Bay connected to the lake. The first two principal components accounted for 77 and 13%, respectively, of the variance in the spectral data.

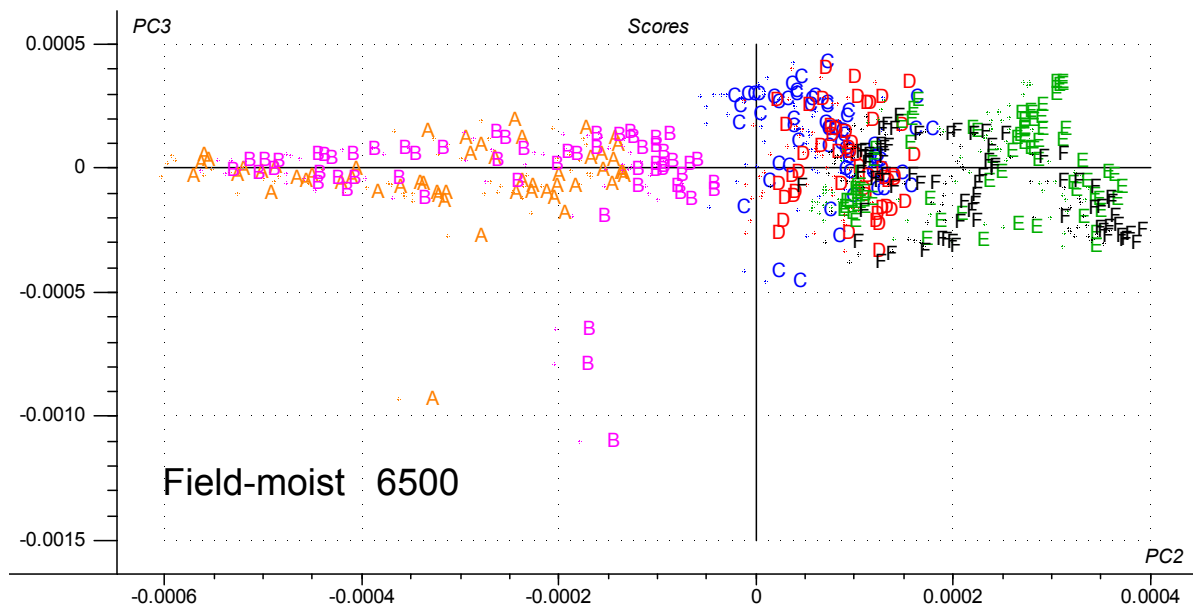


Fig. 29. The same plot as in Fig. 22 except that the scores are plotted on the second and third PCs. The second and third PCs account for 13 and 8%, respectively, of the variance in the spectral data.

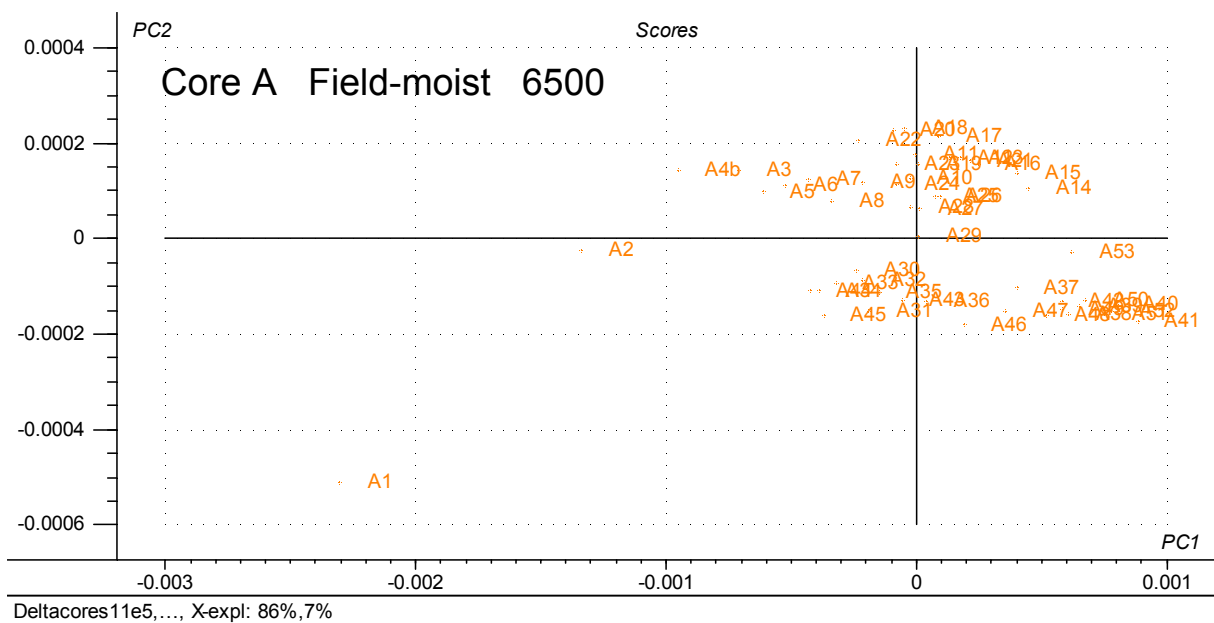


Fig. 30. Scores plot for the 53 samples from core A from Crescent Pond on the first two principal components explaining the variability in the spectral data (600-2498 nm). The spectra were recorded using the model 6500 spectrophotometer and the samples were in moist, "as is" state. The spectral were smoothed and transformed to the second derivative.

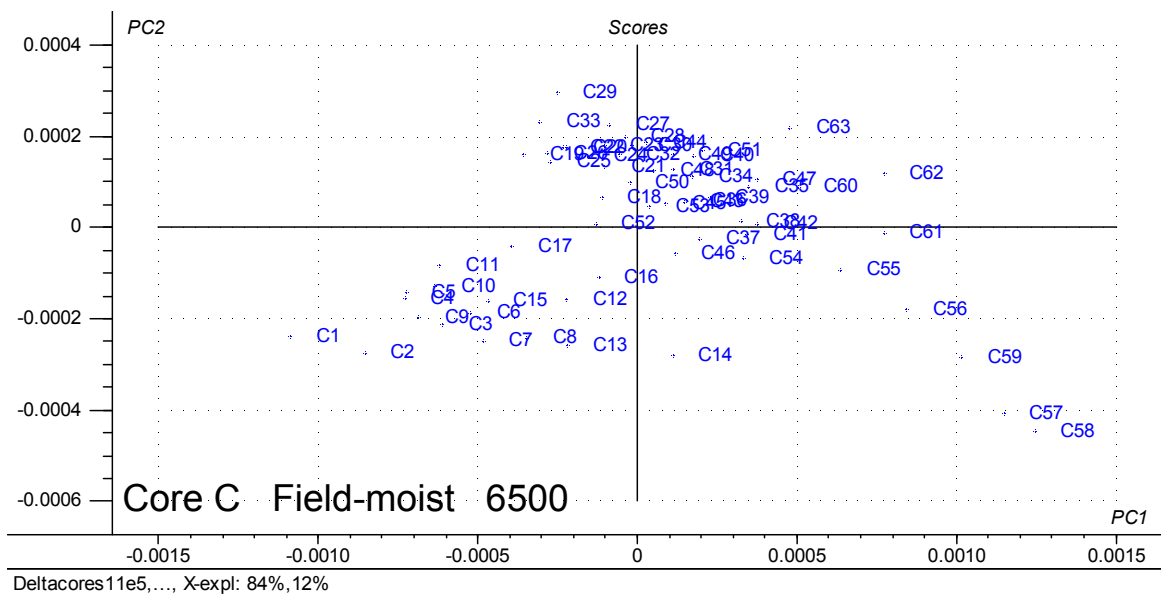


Fig. 31. Scores plot for the 63 samples from core B from Eaglenest on the first two principal components explaining the variability in the spectral data (600-2498 nm). The spectra were recorded using the model 6500 spectrophotometer and the samples were in moist, "as is" state. The spectral were smoothed and transformed to the second derivative.

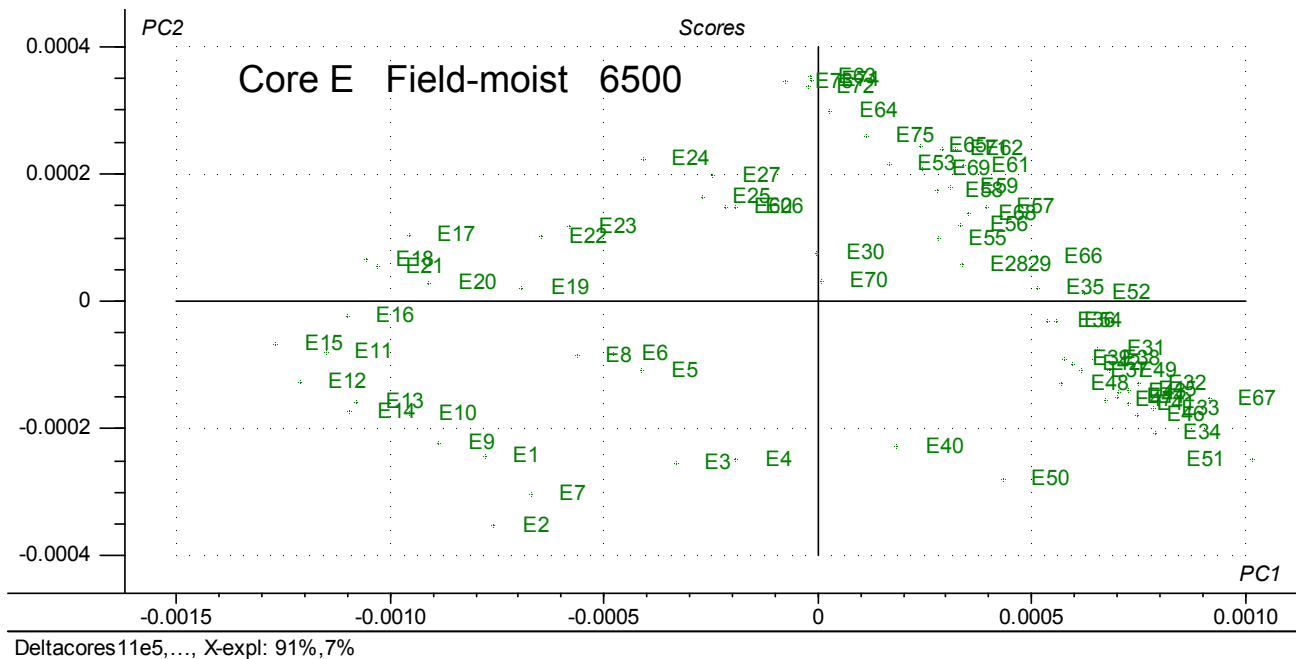


Fig. 32. Scores plot for the 75 samples from core E from Cadham Bay on the first two principal components explaining the variability in the spectral data (600-2498 nm). The spectra were recorded using the model 6500 spectrophotometer and the samples were in moist, "as is" state. The spectral were smoothed and transformed to the second derivative.

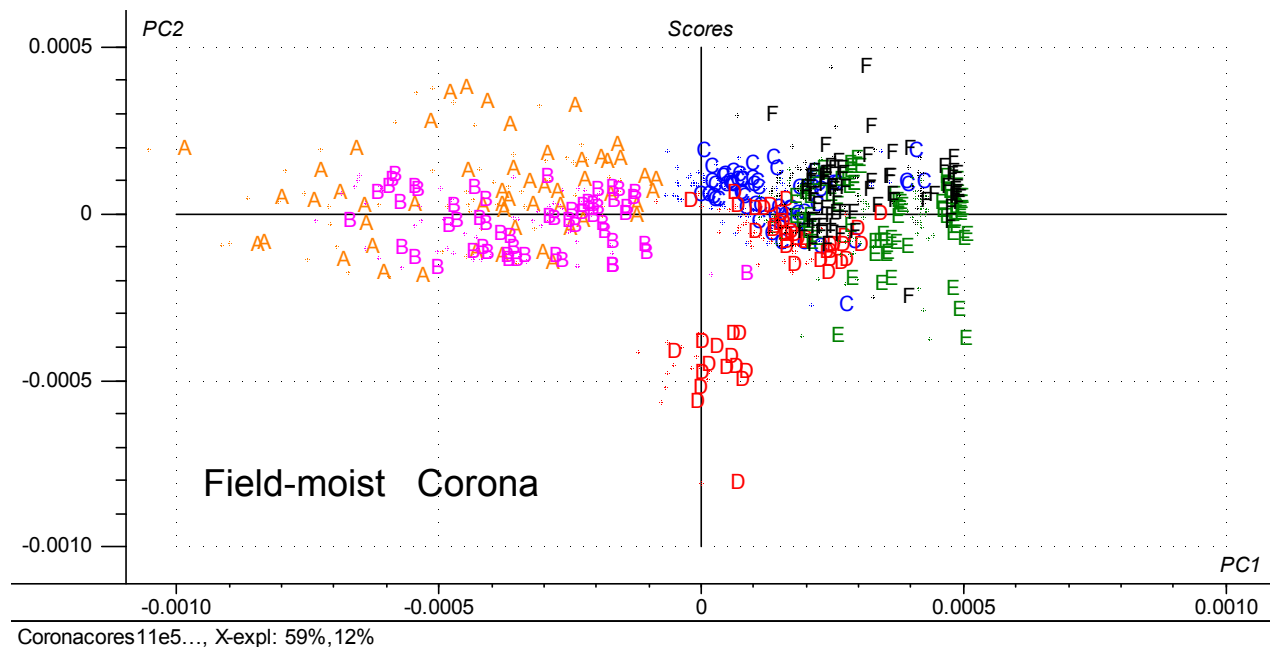


Fig. 33. Scores plot for the 371 samples from the six cores in this study on the first two principal components explaining the variability in the spectral data (426-1600 nm). The spectra were recorded using the Corona and the samples were in moist, "as is" state. The spectral were smoothed and transformed to the second derivative. The cores were A and B from Crescent Pond, C and D from Eaglenest, and E and F from Cadham Bay. The first two principal components accounted for 59 and 12%, respectively, of the variance in the spectral data.

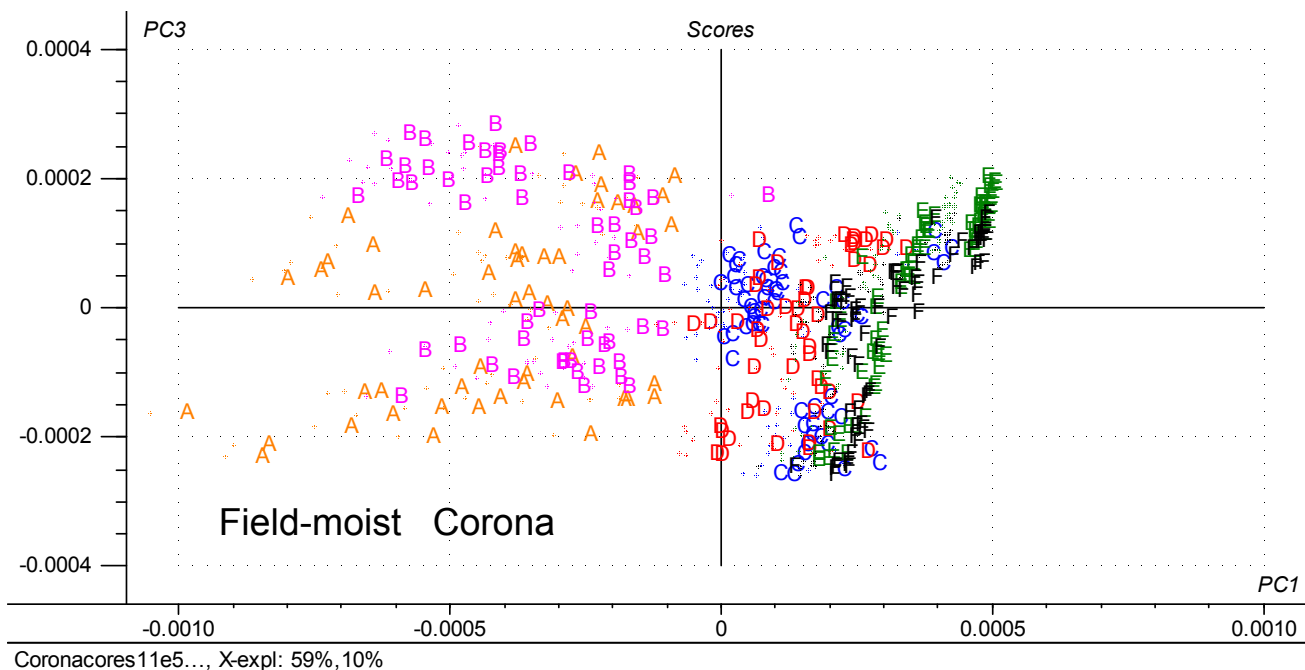


Fig. 34. The same plot as in Fig. 29 except that the scores are plotted on the first and third PCs. The third PC accounts for 10% of the variance in the spectral data.

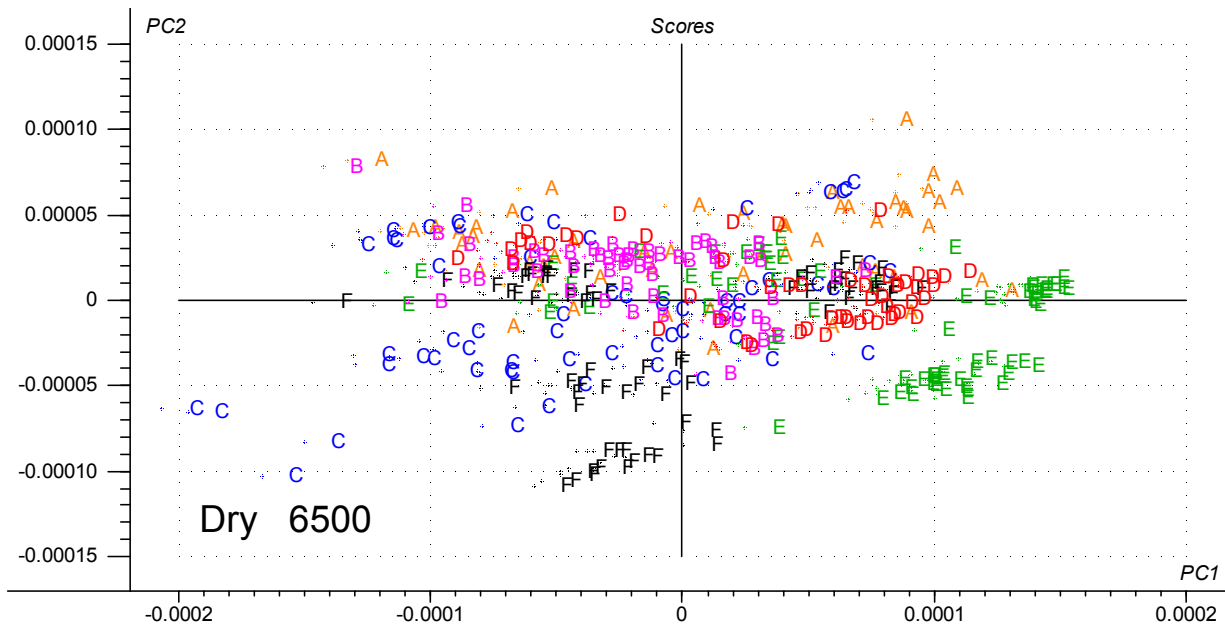


Fig. 35. Scores plot for the 371 samples from the six cores in this study on the first two principal components explaining the variability in the spectral data (1100-2498 nm) recorded using the 6500. The spectra were recorded using the model 6500 spectrophotometer and the samples were dried and ground. The spectra were smoothed and transformed to the second derivative. The first two principal components accounted for 67 and 18%, respectively, of the variance in the spectral data.

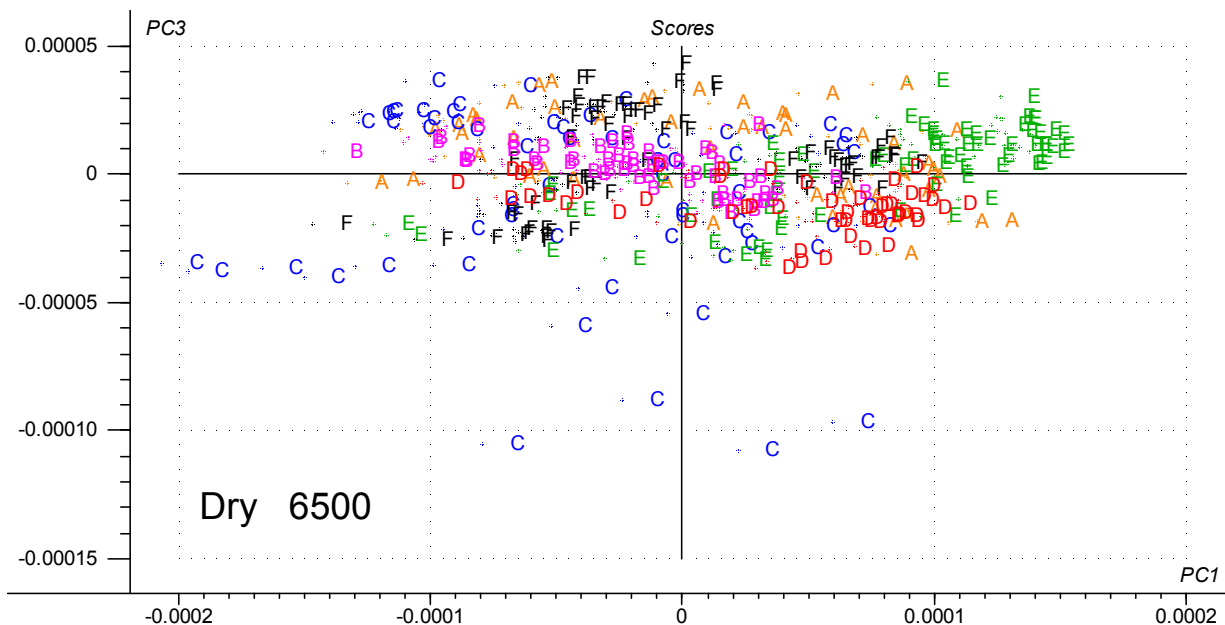


Fig. 36. The same plot as in Fig. 30 except that the scores are plotted on the first and third PCs. The first and third PCs account for 67 and 6%, respectively, of the variance in the spectral data.

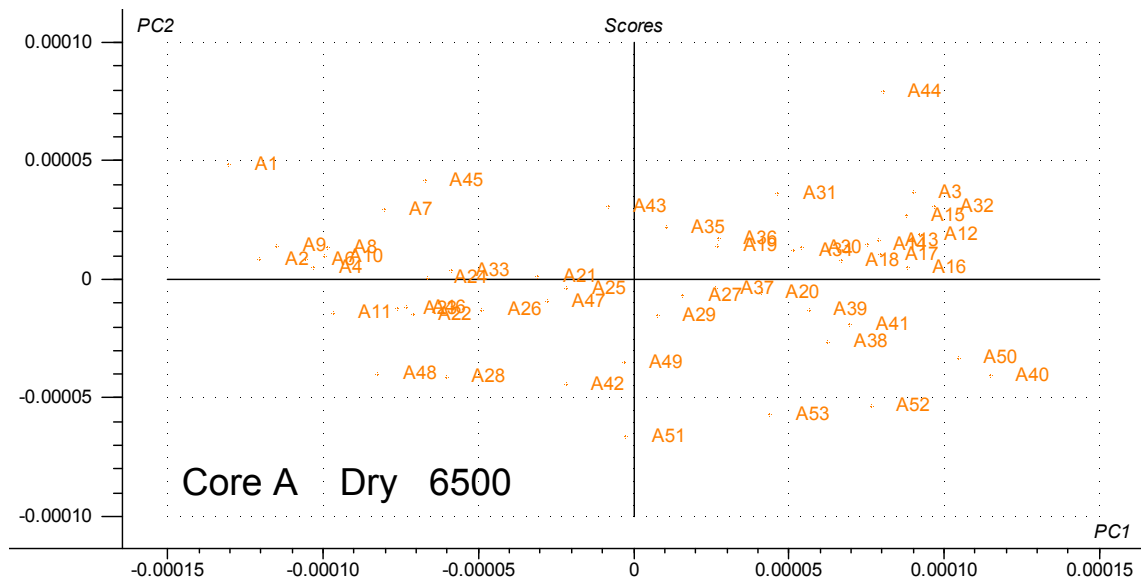


Fig. 37. Scores plot for the 53 samples from core A from Crescent Pond on the first two principal components explaining the variability in the spectral data (1100-2498 nm). The spectra were recorded using the model 6500 spectrophotometer and the samples were dried and ground. The spectral were smoothed and transformed to the second derivative.

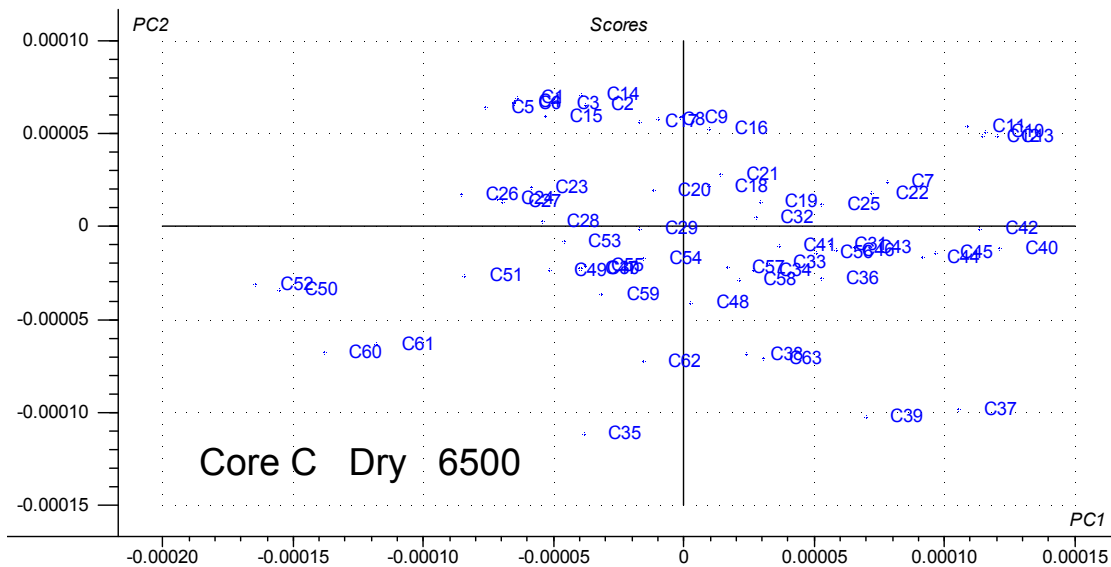


Fig. 38. Scores plot for the 63 samples from core B from Eaglenest on the first two principal components explaining the variability in the spectral data (1100-2498 nm). The spectra were recorded using the model 6500 spectrophotometer and the samples were dried and pulverized. The spectral were smoothed and transformed to the second derivative.

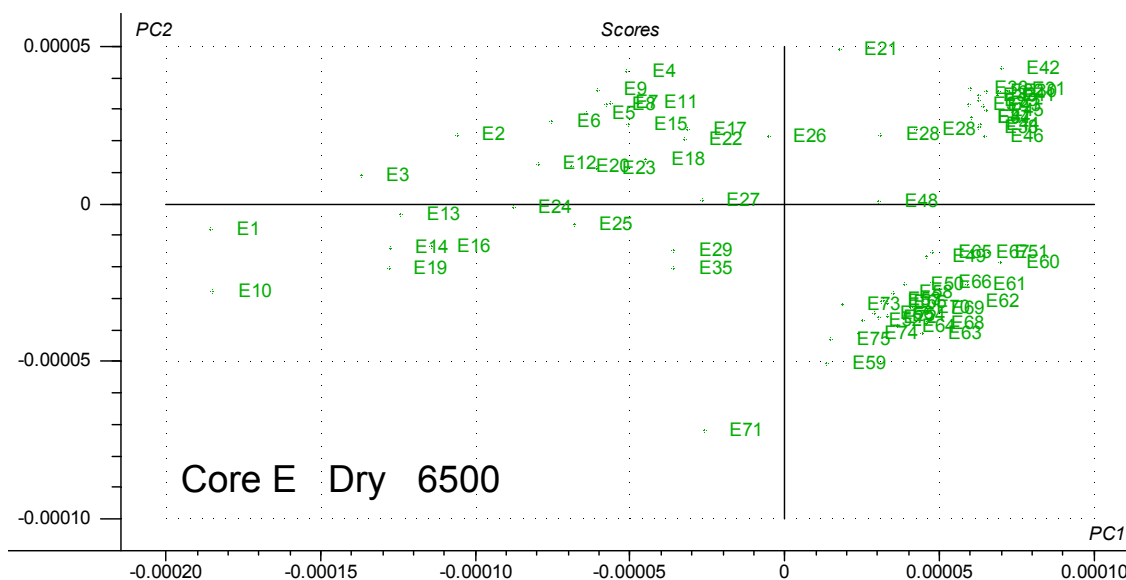


Fig. 39. Scores plot for the 75 samples from core E from Cadham on the first two principal components explaining the variability in the spectral data (1100-2498 nm). The spectra were recorded using the model 6500 spectrophotometer and the samples were dried and pulverized. The spectral were smoothed and transformed to the second derivative.

NIR Prediction of Moisture and Carbon in Cores

Calibrations developed for moisture in the six cores were judged "excellent" for both NIR instruments (Table 3). The NIR-predicted moisture contents agreed ~ 93% with the reference values obtained by oven drying and RPDs were 4 or close to 4. Fig. 40 shows that the relationship between the NIR-predicted moisture values and the reference values was a linear relationship and that results were highly similar between the 6500 and the Corona.

Figures 41 to 44 show the calibration results for C for dry and field-moist samples scanned with the 6500 and the Corona. The calibration based on 6500 spectra for dry samples was "excellent" and that for the Corona for dry samples was "successful". Both calibrations for moist samples were "moderately successful". Figure 45 shows for Core A dry samples that the NIR-predictions modeled the reference data well, including peaks of C content.

Table 3. Accuracy of predictions for NIR calibrations in 370 samples for moisture and 192 samples for C from six cores in this study.

Statistic	Moisture		Carbon			
	6500	Corona	6500		Corona	
	Wet	Wet	Dry	Wet	Dry	Wet
Wavelength Range	630 - 2498	434 - 970, 990 -1634	1100-2498	400-2498	434 - 970, 990 -1634	434 - 1634
r ²	0.927	0.938	0.953	0.857	0.898	0.867
SEP ¹	3.89	3.66	5.32	2.81	7.46	2.68
RPD ¹	3.69	4.02	4.61	2.80	3.28	2.93
RER ¹	20.01	19.44	22.91	14.96	16.35	15.65
a ²	4.55	3.10	0.49	4.27	7.18	4.27
b ³	0.940	0.914	0.995	0.869	0.903	0.869
Math ⁴	Log 1/R	Log 1/R	First derivative	Second derivative	Second derivative	First derivative
Gap ⁵			21	41	41	11
Seg ⁶	21	21	5	41	41	21

¹SEP, RPD and RER are defined in the text.

²a is the y-intercept of the linear regression line, $y = a + bx$, fitted to the x,y points for each of the 6500 and Corona predictions where x values are reference values, and y values are NIR-predicted values.

³b is the slope of the linear regression line, $y = a + bx$, fitted to the x,y points for each of the 6500 and the Corona predictions.

⁴Math is the mathematical pretreatment of the spectral data before the calibration is performed. For moisture, the raw spectral data expressed as $\log 1/R$ where R is reflectance, were used without transformation to first or second derivative.

⁵Gap is the number of wavelength points over which the derivative is taken where wavelength points are 2 nm apart.

⁶Seg is the number of wavelength points over which the spectral data were smoothed.

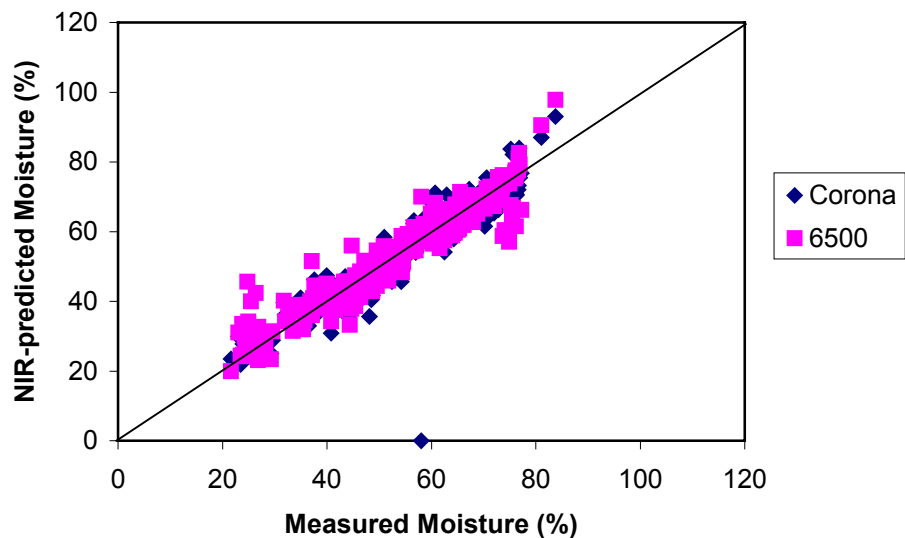


Fig. 40. Linear regression relationships between the NIR-predicted values for moisture and those determined by oven drying for two NIR instruments. Calibration performance and linear regression statistics are given in Table 3.

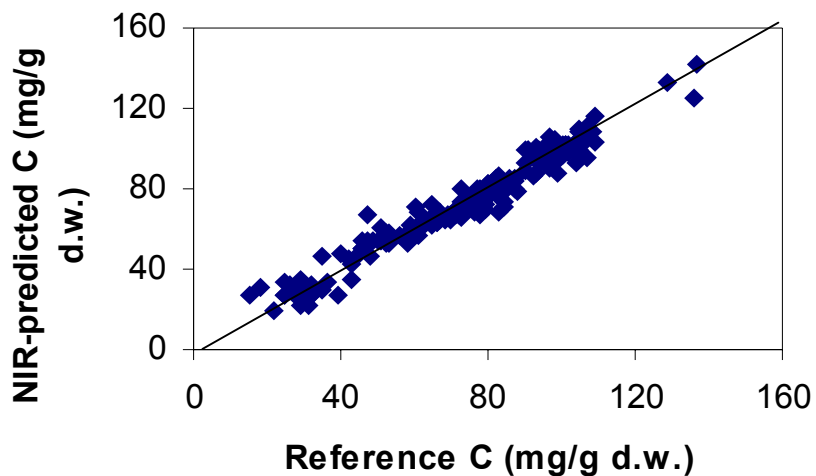


Fig. 41. Linear regression relationships between the NIR-predicted values for C and reference values determined by combustion on dried, ground samples. Scans were performed with the Foss NIRSystems model 6500. Calibration performance and linear regression statistics are given in Table 3.

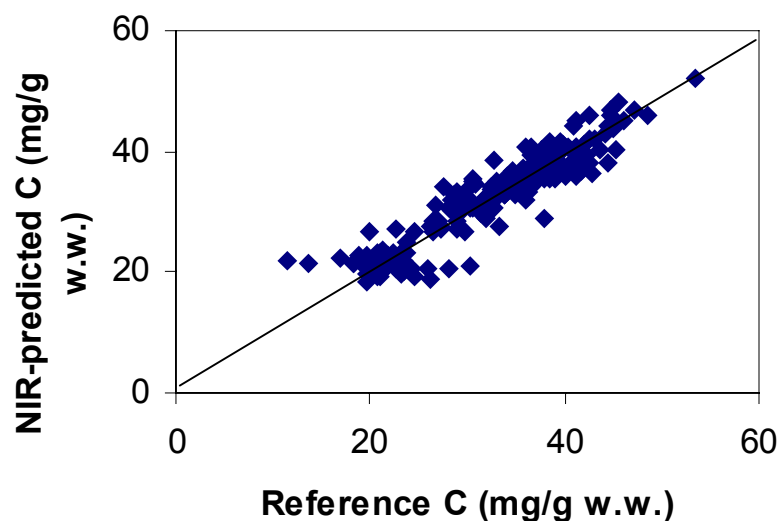


Fig. 42. Linear regression relationships between the NIR-predicted values for C and C determined by combustion and expressed on a wet weight basis. Scans were performed on field-moist samples with the Foss NIRSystems model 6500. Calibration performance and linear regression statistics are given in Table 3.

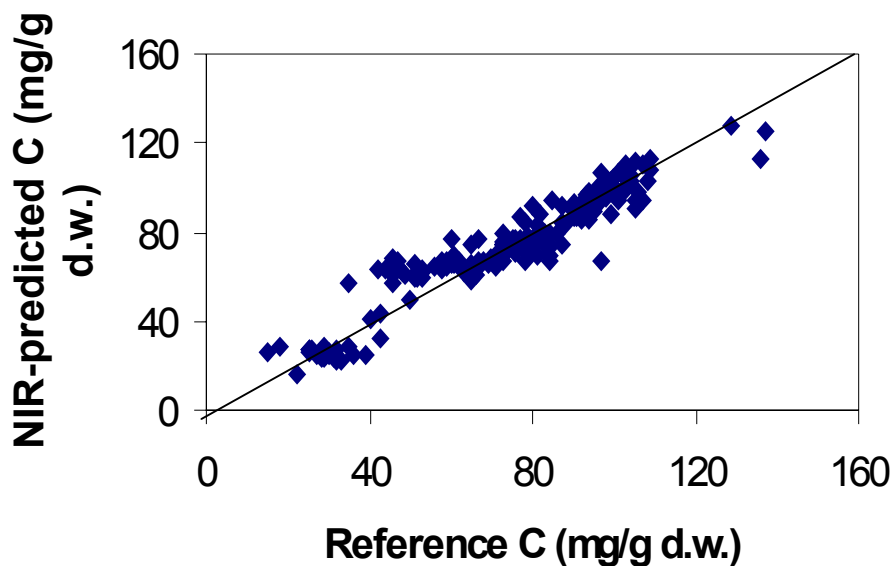


Fig. 43. Linear regression relationships between the NIR-predicted values for C and those determined by combustion in dry, ground samples. Scanning was performed on the Zeiss Corona. Linear regression statistics are given in Table 3.

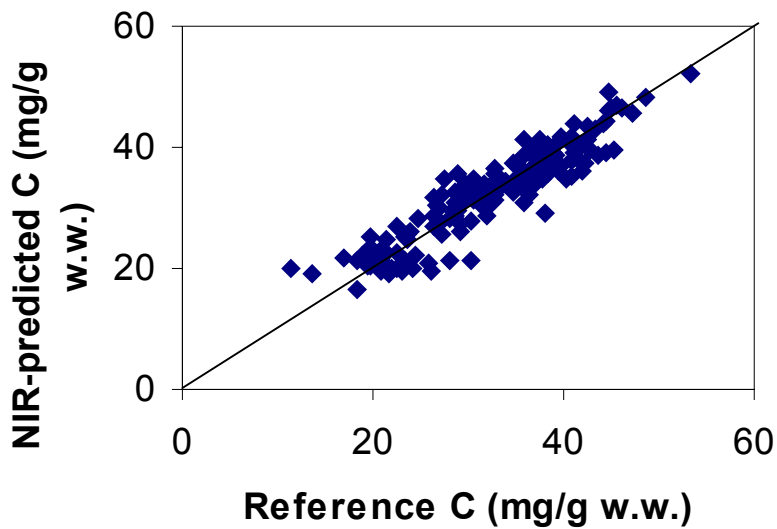


Fig. 44. Linear regression relationships between the NIR-predicted values for C and C determined by combustion and expressed on a wet weight basis. Scans were performed on field-moist samples with the Zeiss Corona. Calibration performance and linear regression statistics are given in Table 3.

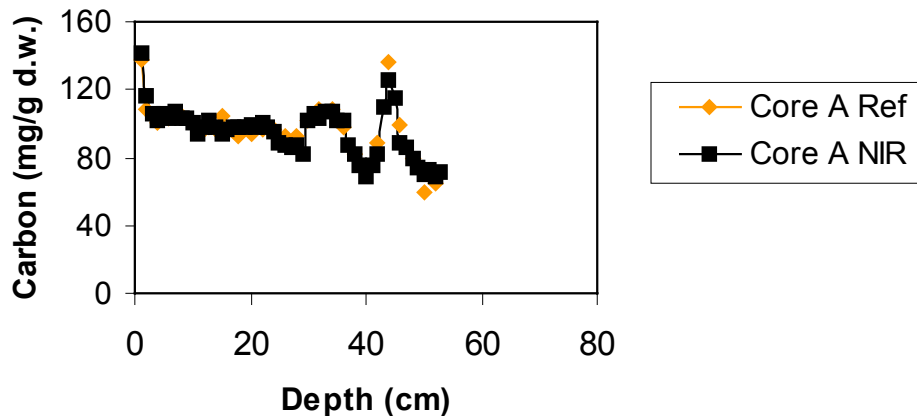


Fig. 45. Comparison of reference values and NIR-predicted values for C determined using the 6500 spectra from dry samples for Core A profile

Estimation of Carbon per Unit Area

The results of calculating C as g cm^{-3} in the six cores are graphed in Fig. 46 and tabulated in Appendix I. Values for all of the 371 samples are NIR-predicted. Generally, the content of C was greatest in the "as is", field-moist cores between about 20 and 50 cm depth. Duplicate cores from each site showed similar profiles. The profiles for Crescent Pond and Eaglenest were very similar whereas the profile for Cadham showed lower C content than the other sites between the surface and 30 cm. All the sites were similar in C content below 30 cm.

The total C contained in cores A to F determined using the 6500 was 2.51, 2.79, 2.99, 2.49, 3.24, and 2.87 g cm^{-2} , respectively. Since the cores varied in length, C per unit area was dependent in part on core length. The total C calculated for slices 2 to 51 cm, common to all cores, was 2.42, 2.43, and 2.06 g cm^{-2} , respectively, for Crescent, Eaglenest and Cadham. This is consistent with the information in Fig. 46 that Crescent and Eaglenest were highly similar in C profiles, and that Cadham contained lower C content in profile above 50 cm.

The results for C per unit area for each core were very similar between the 6500 and Corona NIR instruments. The coefficients of variability (deviation as a % of the mean) between the results from the two instruments for cores A to F were 2.74, 0.50, 0.20, 1.38, 0.37, and 0.05%, respectively.

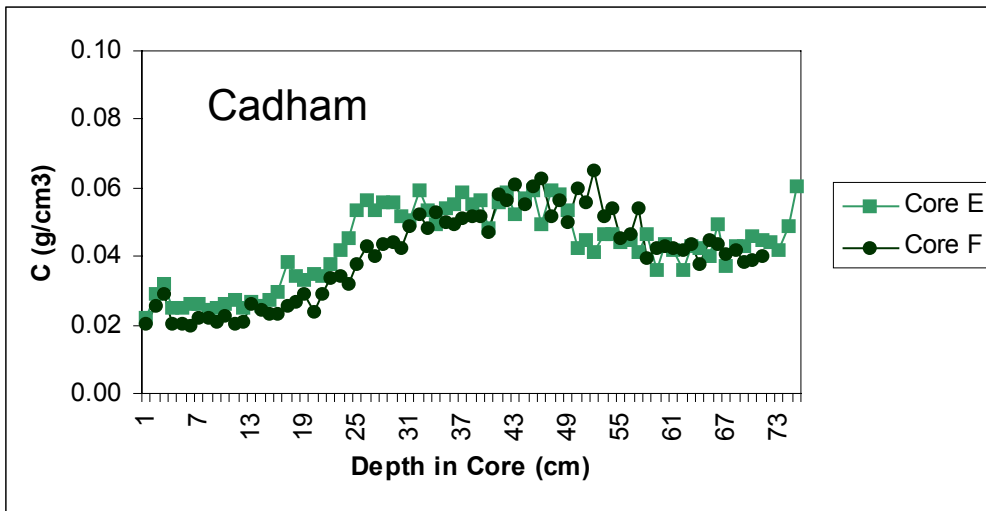
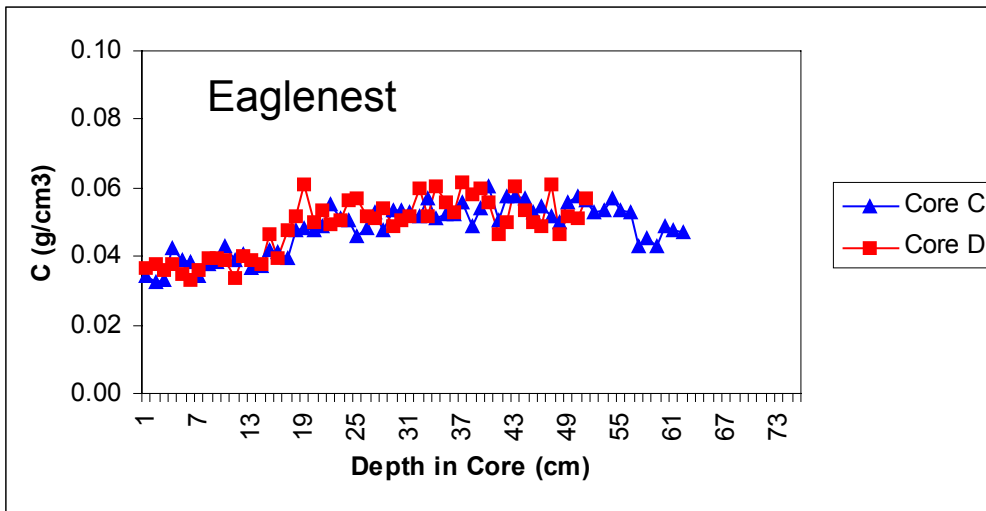
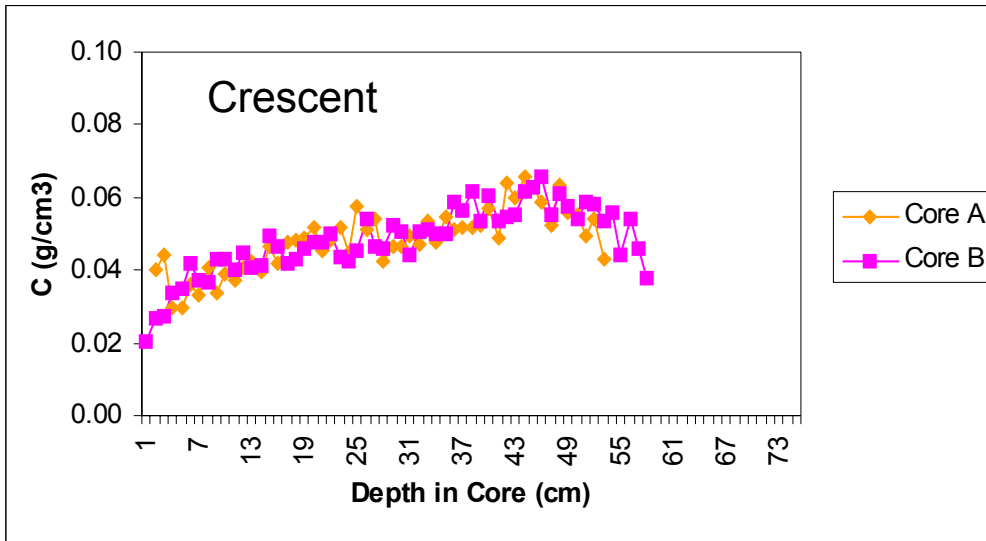


Fig. 46. Profiles of total C in the six cores in this study predicted from spectra of field-moist samples scanned with the Foss NIRSystems 6500 NIR instrument.

Discussion

Effectiveness of the Sampling

The purpose of this study was to develop a rapid, cost-effective method of using NIRS for estimating the quantity of total C as g cm^{-2} in several representative sites in Delta Marsh. This depended upon obtaining cores that contained the full depth of stored organic carbon in the marsh. Ranging from 71 to 75 cm in length, the Cadham Bay cores in the present study did not reach the ~ 100 cm length identified by Sproule (1972) as representing the full record of the 2400 y history of the marsh. The cores in the 1972 study were comprised of silty clays and silty sands and the ones in the present study appear to be of a similar nature. It is probable that cores E and F were sampled close to the location in Cadham Bay sampled by Sproule (1972). It is likely they do not represent all of the history of the marsh. Extrapolating cores E and F to 100 cm length, assuming that the C content of slices 75 to 100 cm is 0.04 g, results in estimates of 4.03 and 4.24 g of C g cm^{-2} , respectively, for Cadham Bay.

The cores in the present study were collected through the ice by hand by inserting the core tube into the sediment until it met with resistance. Power-assisted sampling methods may be required to obtain longer cores representing the full paleological record.

There is no direct information on how deep the record of stored carbon is at the other two sites or how much of the paleological record is captured in them. In the future, it would be desirable to date cores from representative marsh sites by Pb^{210} or another method to ensure that the full history and C accumulation of the marsh is captured.

Qualitative Differences Among and Within Cores

The spectra from samples contain information about their composition and functional properties. Information can be retrieved by statistical analysis of the spectra, as performed here using principal component analysis. This analysis showed that the sediments sampled from the larger water bodies, Eaglenest and Cadham Bay, were more similar to each other than to those from the small, shallow Crescent Pond (Fig. 23, 24). This may not be unexpected since both Eaglenest and Cadham Bay, by Delta Marsh standards, were relatively large and deep water bodies. Information on changes in quality down the cores are shown for three of the cores in Fig. 30 to 32 in two-dimensional space but a three-dimensional representation would be easier to visualize. When the field-moist samples were analyzed, the first several samples tended to be at one extreme of PC1. Progressing down the core, samples moved to the other side of the plot. With overall moisture content from 22 to 84% and with the OH of water being the prominent absorber in the NIR region, it is expected that PC1 is dominated by water. Separation of sites along PC1 in Fig. 28 and 29 probably reflects that the Crescent Pond samples were wetter than those from Eaglenest and Cadham.

More significant information, such as about C content, organic matter content, or quality, may be gained from the dry samples where the free water removed. Figures 35 and 36 show less separation of Crescent samples from those from the other two sites supporting the conclusion that water was dominant in PC1 in the analysis of field-moist samples. Nevertheless, there is some separation of sites, shown by groups of samples from cores A, C, E, and F that are not-overlapping with other

cores. This information can be used in a large-scale study of a marsh for the selection of samples to be analyzed chemically and used in calibrations to predict the rest of the samples. If numerous cores were collected in a marsh by grid, transect or stratified sampling, all cores need only be sectioned, dried and scanned. The PCA on all samples permits the selection of representative cores, that cover the full range of variability in matrix (spectral) quality, for chemical analysis. In this way, the NIR calibrations developed are better able to accurately predict constituents in all cores in the study. The result is that all samples collected in the study can be analyzed for constituents of interest without the need for costly chemical analyses.

In addition to cost-effective analysis of C within the marsh, NIR can assist in identifying samples of potential paleolimnological interest vertically down the core. Regions of spectral change are likely to provide information about conditions during deposition. For example, Fig. 37 shows that samples A1 and A2 (0-1 and 1-2 cm, respectively) at the left hand end of PC1 were reasonably similar, whereas A3 was at the right hand end of PC1. Below A3, samples clustered around A2. Sample A3 would be a subject for analysis separate from A2 and A4 since it differed from the trend. Samples A13 to A 18 clustered together, making it likely that only one or two these need be analyzed. In this study, core slices were 1 cm, but cores could be sliced into thinner sections and still be amenable to NIR analysis, if required for more detailed paleolimnological analysis.

To our knowledge this is one of the first studies using NIRS for the analysis of soils from a lacustrine wetland. An earlier student project examined the analysis of C and N in short cores from drier areas of Delta Marsh (Mathias 2000). Soils were sampled to a maximum of 20 cm depth from each of three of the dominant plant communities, the common reedgrass, *Phragmites australis*, whitetop, *Scolochloa festucacea*, and the cattail, *Typha glauca*. The PCA of the samples from this study together with those from Mathias (2000) shows that there is little overlap between the samples taken from the emergent plant communities and the samples taken from the bottom of the water bodies (Fig. 47). The semi-terrestrial samples were more diverse than those from the present study. The samples are distributed along the PC1 axis from left to right from semi-terrestrial towards increasingly aquatic environments, i.e., emergents, wet meadow areas, small shallow Crescent Pond, aquatic Eaglenest with no connection to Lake Manitoba, and Cadham Bay with a substantial connection to Lake Manitoba. It appears that PC1 is related to the content and/or quality of vegetative remains. The short core samples to the left of the plot contain roots and decaying vegetation whereas the long cores to the right of the plot are geologically older, will have low contents of more highly degraded C.

Quantitative Analysis of Moisture and Carbon

Using the statistical evaluation criteria proposed here, results for moisture were "excellent" and for C were "moderately successful" to "excellent" with both NIR instruments. The method of slicing cores, analyzing selected dried samples for C, and using the resulting data as reference data to calibrate NIR spectra is a feasible method for cost-effective analysis of numerous field-moist samples from wetlands to determine the C inventory.

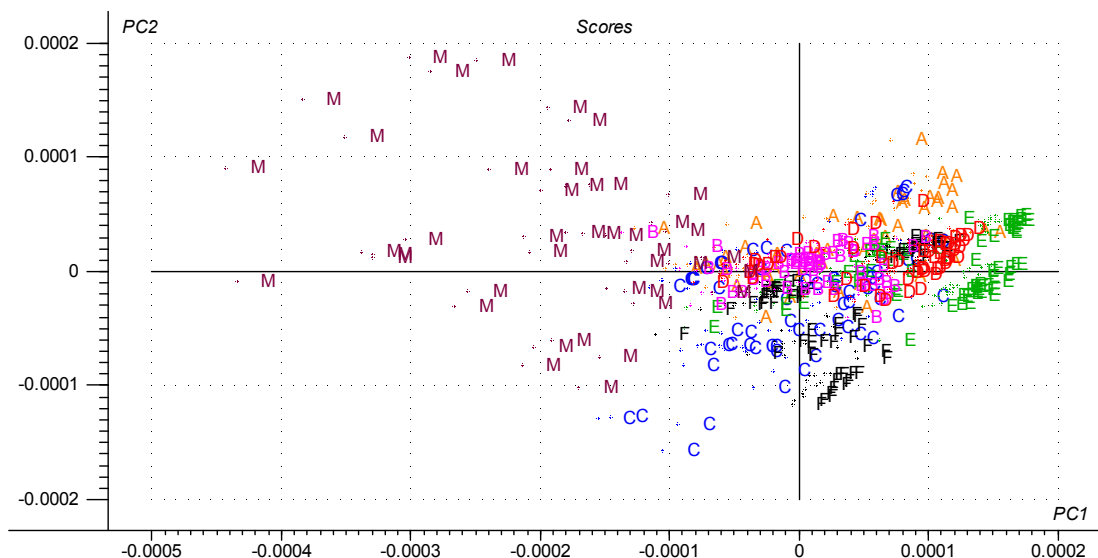


Fig. 47. Scores plot for the 371 samples from the six cores in this study and 42 samples from the Mathias (2000) on the first two principal components explaining the variability in the spectral data (1120-2478 nm). The spectra were recorded using the 6500 and the samples were dried and pulverized or ground. The spectra were smoothed and transformed to the second derivative. The cores were A and B from Crescent Pond, C and D from Eagenest, E and F from Cadham Bay, and M from the Mathias study. The first two principal components accounted for 73 and 15%, respectively, of the variance in the spectral data.

The Potential for Near-infrared Spectroscopy for On-site Determination of Carbon Inventory in Wetlands and Peatlands

This study suggests that NIRS is a good candidate for a method for the quantitative determination of C in wetlands on a landscape basis. Moreover, the method can potentially be used on-site in the field. This study demonstrated that the field-portable Corona NIR instrument provided virtually identical results for C inventories in the cores as did the widely-used benchtop 6500 instrument. Taking the instrument to the field would avoid most of the costs in time and money associated with packaging, labeling, transport, and storage of samples. Nevertheless, a portion of samples measured by NIRS must always be checked by reference analysis. Most of the time and money spent for laboratory analysis of samples would be avoided.

From the standpoint of stored C in Canada, peatlands are the wetlands are of prime significance. Several NIR studies have been performed on peat. An 80-cm peat core of the blanket bog of Moor House National Reserve, Great Britain, was sectioned, dried, and ground. Successful calibrations were developed for moisture, bulk density, degree of humification, identifiable *Sphagnum*, unidentified organic material, and remains of several plant species (McTiernan et al. 1998). Beining et al. (2001) predicted gross heat, C, cellulose, H, N, and ash successfully in freeze-dried peat from Irish bogs. Downey and Byrne (1986) predicted moisture and bulk density in milled peat, with moisture range 34 to 71%, using NIRS. NIR-predicted data agreed 99% for moisture and 94% for bulk density with the measured values.

Nilsson et al. 1993 scanned samples of peat and correlated the spectral data with anaerobic methane generation by methanogenic bacteria from the same samples. Up to 84 % of the variance in methane production rates were explained using the NIR spectra. Thus, NIRS has potential for measuring the release of carbon dioxide and methane from wetlands.

While most work with NIRS has been done on dried samples, Downey and Bryne (1986) and Nilsson et al. (1993) used moist peat samples. Malley et al. (2000) compared predictive results with field-moist and dried soil and found that while some determinations on the moist soil were satisfactory, in general, better results were obtained with dry soil.

In conclusion, NIRS is a feasible method for the determination of C inventories in wetlands when combined with effective sampling of the full depth of the organic C layer, appropriate sampling of spatial variability of the depth of the organic layer within representative habitats of the wetland, and measurement of areal extent of the representative habitats. It is expected that the technique can be utilized in peatlands as well as lacustrine wetlands. Field-portable NIRS instruments are presently available, such as the Zeiss Corona used in the present study, that can further reduce cost, time and effort and increase efficiency.

References

- Beining, B.A., N.M. Holden, S.M. Ward, and E.P. Farrell. 2001. The prediction of some peat properties for Irish industrial bogs using near infrared spectroscopy (unpublished). <http://www.bnm.ie/downloads/beining.pdf>
- Ben-Dor, E. 2002. Quantitative remote sensing of soil properties. *Advances in Agronomy*, Vol 75: 173-243.
- Ben-Dor, E., Y. Inbar, and Y. Chen. 1997. The reflectance spectra of organic matter in the visible near-infrared and short wave infrared region (400-2500 nm) during a controlled decomposition process. *Remote Sens. Environ.* 61:1-15.
- Confalonieri, M., F. Fornasier, A. Ursino, F. Boccardi, B. Pintus, and M. Odoardi. 2001. The potential of near infrared reflectance spectroscopy as a tool for the chemical characterisation of agricultural soils. *J. Near Infrared Spectrosc.* 9: 123-131.
- Dalal, R.C. and R.J. Henry. 1986. Simultaneous determination of moisture, organic carbon, and total nitrogen by near infrared reflectance spectrophotometry. *Soil Sci. Soc. Am. J.* 50: 120-123.
- Downey, G. and P. Bryne. 1986. Prediction of moisture and bulk density in milled peat by near infrared reflectance. *J. Sci. Food Agr.* 37: 231-238.
- Gillon, D., R. Joffre and P. Dardenne. 1993. Predicting the stage of decay of decomposing leaves by near infrared reflectance spectroscopy. *Can. J. For. Res.* 23: 2552-2559.
- Joffre, R., D. Gillon, P. Dardenne, R. Agneessens and R. Biston. 1992. The use of near-infrared reflectance spectroscopy in litter decomposition studies. *Ann. Sci. For.* 49: 481-488.
- Ludwig, B. and P.K. Khanna. 2001. Use of near infrared spectroscopy to determine inorganic and organic carbon fractions in soil and litter. Chapter 25, pp 361-370. Eds. R. Lal, J. M Kimble, R.F. Follett, B.A. Stewart. *Assessment Methods for Soil Carbon*. Adv. Soil Sci. Lewis Publishers, Boca Raton.
- Malley, D.F., L. Lockhart, P. Wilkinson, and B. Hauser. 2000. Determination of carbon, carbonate, nitrogen, and phosphorus in freshwater sediments by near-infrared reflectance:

- rapid analysis and a check on conventional analytical methods. *Journal of Paleolimnology* 24: 415-425.
- Malley, D.F., H. Röncke, D.L. Findlay, and B. Zippel. 1999. Feasibility of using near-infrared reflectance spectroscopy for the analysis of C, N, P, and diatoms in lake sediments. *Journal of Paleolimnology* 21: 295-306.
- Malley, D.F., B. Trybula, R.D. Ross, and G. Gay. 2000. Evaluating the use of near-infrared spectroscopy for the analysis of biosolids constituents. Project 99-PUM-6-ET, Water Environment Research Foundation, Alexandria, VA. D00306WW
- Mathias, L. 2000. Exploring the use of near-infrared spectroscopy for estimating carbon stores in wetland soils. International Baccalaureate Extended Essay, Silver Heights Collegiate, Winnipeg MB, 23 p.
- Martin, P.D., D.F. Malley, G. Manning, and L. Fuller. 2002. Determination of soil organic carbon and nitrogen at the field level using near-infrared spectroscopy. *Can. J. Soil Sci.* 82: 413-422
- McCarty, G.W. and J.B. Reeves 111. 2001. Development of rapid instrumental methods for measuring soil organic carbon. Chapter 26, pp 371-380. Eds. R. Lal, J. M Kimble, R.F. Follett, B.A. Stewart. *Assessment Methods for Soil Carbon*. Adv. Soil Sci. Lewis Publishers, Boca Raton.
- McLellan, T.M, J.D. Aber, M.E. Martin, J.M. Melillo and K.J. Nadelhoffer. 1991. Determination of nitrogen, lignin, and cellulose content of decomposing leaf material by near infrared reflectance spectroscopy. *Can. J. Forest Res.* 21: 1684-1688.
- McLellan T.M, M.E. Martin, J.D. Aber, J.M. Melillo, K.J. Nadelhoffer and B. Dewey 1991. Comparison of wet chemistry and near infrared reflectance measurements of carbon-fraction chemistry and nitrogen concentration of forest foliage. *Can. J. Forest Res.* 21:1689-1693.
- McTiernan, K.B., M.H. Garnett, D. Mauquoy, P. Ineson, and M.-M. Coûteaux. 1998. Use of near-infrared reflectance spectroscopy (NIRS) in paleoecological studies of peat. *The Holocene* 8,6: 729-740.
- Morra, M.J., M.H. Hall and L.L. Freeborn. 1991. Carbon and nitrogen analysis of soil fractions using near-infrared reflectance spectroscopy. *Soil Sci. Soc. Am. J.* 55: 288-291.
- Nilsson, M., T. Korsman, A. Nordgren, C. Palmberg, I. Renberg, and J. Ohman. 1993. NIR spectroscopy used in the microbiological and environmental sciences. p 229-234. In K.I. Hildrum, T. Isaksson, T. Naes, and A. Tandberg (eds.) *Near Infra-red Spectroscopy: Bridging the Gap between Data Analysis and NIR Applications*. Ellis Horwood, New York.
- Pietikainen, J. and H. Fritze. 1995. Clear-cutting and prescribed burning in coniferous forest: Comparison of effects on soil fungal and total microbial biomass, respiration activity and nitrogen. *Soil Biol. Biochem.* 27: 101-109.
- Shay, J. undated. Delta Marsh Ecology, www.wilds.mb.ca/delta
- Sproule, Thomas A. 1972. A paleoecological investigation into the post-glacial history of Delta Marsh, Manitoba. M.Sc. Thesis, Department of Botany, University of Manitoba. 49 pp.
- Statistics Canada. 2000. Human Activity and the Environment 2000. CD Rom, Catalogue No. 11-509-XPS
- Teller, J.T. and W.M. Last 1981. Late Quaternary history of Lake Manitoba, Canada. *Quaternary Research* 16: 97-116.
- The Bureau of the Convention on Wetlands. 2002. The List of Wetlands of International Importance. July. <http://www.ramsar.org/sitelist.pdf>
- Williams, P. and K. Norris (Eds). 2001. *Near-Infrared Technology in the Agricultural and Food Industries*, 2nd Edition, American Association of Cereal Chemists, St. Paul MN, 312 pp.

Appendix I. NIR-predicted C content (g cm^{-3}) in each slice of each of the six cores in this study. Each slice was 1 cm thick. Samples were scanned in the field-moist state on two NIR instruments. Cores A and B, C and D, and E and F were duplicates sampled from each of three sites within Delta Marsh

	Crescent		Crescent		Eaglenest		Eaglenest	
	Core A	Core A	Core B	Core B	Core C	Core C	Core D	Core D
Slice	6500	Corona	6500	Corona	6500	Corona	6500	Corona
1			0.0205	0.0250	0.0343	0.0355	0.0367	0.0377
2	0.0399	0.0453	0.0268	0.0319	0.0326	0.0321	0.0378	0.0412
3	0.0442	0.0478	0.0274	0.0296	0.0333	0.0309	0.0361	0.0356
4	0.0295	0.0307	0.0338	0.0356	0.0424	0.0388	0.0380	0.0354
5	0.0297	0.0319	0.0349	0.0348	0.0389	0.0353	0.0347	0.0332
6	0.0362	0.0381	0.0416	0.0398	0.0385	0.0338	0.0332	0.0307
7	0.0329	0.0342	0.0372	0.0361	0.0344	0.0310	0.0360	0.0330
8	0.0408	0.0431	0.0365	0.0348	0.0375	0.0336	0.0393	0.0373
9	0.0339	0.0363	0.0429	0.0403	0.0382	0.0357	0.0396	0.0375
10	0.0392	0.0409	0.0428	0.0415	0.0430	0.0372	0.0392	0.0364
11	0.0371	0.0367	0.0400	0.0415	0.0388	0.0347	0.0337	0.0314
12	0.0405	0.0403	0.0446	0.0445	0.0405	0.0353	0.0403	0.0367
13	0.0424	0.0425	0.0405	0.0408	0.0369	0.0335	0.0387	0.0369
14	0.0398	0.0392	0.0412	0.0400	0.0373	0.0328	0.0380	0.0355
15	0.0466	0.0469	0.0495	0.0483	0.0419	0.0387	0.0467	0.0431
16	0.0418	0.0419	0.0463	0.0442	0.0411	0.0382	0.0397	0.0365
17	0.0478	0.0464	0.0417	0.0395	0.0397	0.0366	0.0477	0.0449
18	0.0483	0.0467	0.0430	0.0412	0.0475	0.0462	0.0519	0.0483
19	0.0486	0.0506	0.0458	0.0431	0.0485	0.0463	0.0612	0.0569
20	0.0516	0.0501	0.0478	0.0460	0.0474	0.0462	0.0502	0.0490
21	0.0453	0.0420	0.0476	0.0431	0.0486	0.0465	0.0535	0.0512
22	0.0484	0.0477	0.0501	0.0474	0.0553	0.0528	0.0495	0.0468
23	0.0516	0.0524	0.0439	0.0428	0.0512	0.0495	0.0508	0.0486
24	0.0449	0.0453	0.0427	0.0415	0.0506	0.0499	0.0564	0.0546
25	0.0578	0.0602	0.0454	0.0435	0.0460	0.0440	0.0572	0.0549
26	0.0510	0.0545	0.0540	0.0512	0.0480	0.0475	0.0516	0.0512
27	0.0538	0.0585	0.0465	0.0445	0.0529	0.0514	0.0509	0.0486
28	0.0425	0.0470	0.0459	0.0447	0.0479	0.0488	0.0541	0.0510
29	0.0464	0.0512	0.0524	0.0518	0.0536	0.0533	0.0488	0.0460
30	0.0465	0.0526	0.0503	0.0494	0.0536	0.0531	0.0507	0.0469
31	0.0492	0.0633	0.0443	0.0439	0.0529	0.0521	0.0515	0.0498
32	0.0468	0.0524	0.0506	0.0517	0.0519	0.0486	0.0601	0.0580
33	0.0536	0.0644	0.0512	0.0522	0.0573	0.0550	0.0518	0.0498
34	0.0476	0.0566	0.0503	0.0511	0.0509	0.0483	0.0604	0.0585
35	0.0547	0.0643	0.0498	0.0492	0.0526	0.0507	0.0559	0.0550
36	0.0510	0.0623	0.0589	0.0585	0.0522	0.0497	0.0532	0.0526

	Core A	Core A	Core B	Core B	Core C	Core C	Core D	Core D
Slice	6500	Corona	6500	Corona	6500	Corona	6500	Corona
37	0.0516	0.0611	0.0567	0.0552	0.0561	0.0556	0.0615	0.0614
38	0.0515	0.0600	0.0619	0.0611	0.0491	0.0458	0.0583	0.0564
39	0.0525	0.0599	0.0533	0.0537	0.0543	0.0530	0.0601	0.0596
40	0.0570	0.0587	0.0605	0.0612	0.0603	0.0593	0.0558	0.0547
41	0.0488	0.0501	0.0534	0.0536	0.0507	0.0493	0.0464	0.0497
42	0.0638	0.0654	0.0544	0.0536	0.0573	0.0590	0.0502	0.0521
43	0.0599	0.0624	0.0552	0.0548	0.0577	0.0593	0.0607	0.0602
44	0.0658	0.0677	0.0617	0.0607	0.0569	0.0590	0.0533	0.0537
45	0.0628	0.0657	0.0630	0.0610	0.0532	0.0541	0.0499	0.0483
46	0.0590	0.0627	0.0658	0.0671	0.0544	0.0582	0.0487	0.0508
47	0.0524	0.0548	0.0553	0.0552	0.0519	0.0526	0.0609	0.0631
48	0.0635	0.0659	0.0610	0.0604	0.0497	0.0522	0.0466	0.0473
49	0.0557	0.0552	0.0578	0.0571	0.0558	0.0582	0.0519	0.0505
50	0.0549	0.0522	0.0539	0.0536	0.0575	0.0604	0.0514	0.0514
51	0.0492	0.0468	0.0585	0.0582	0.0566	0.0598	0.0571	0.0595
52	0.0541	0.0528	0.0580	0.0581	0.0530	0.0593		
53	0.0431	0.0402	0.0534	0.0528	0.0533	0.0586		
54			0.0555	0.0561	0.0572	0.0610		
55			0.0443	0.0451	0.0536	0.0570		
56			0.0542	0.0535	0.0531	0.0546		
57			0.0462	0.0465	0.0432	0.0489		
58			0.0379	0.0394	0.0452	0.0524		
59					0.0433	0.0507		
60					0.0488	0.0549		
61					0.0478	0.0535		
62					0.0473	0.0534		
63								
64								
65								
66								
67								
68								
69								
70								
71								
72								
73								
74								
75								
Total, g	2.508	2.646	2.791	2.763	2.986	2.974	2.488	2.419

	Cadham Cadham		Cadham Cadham	
	Core E	Core E	Core F	Core F
Slice	6500	Corona	6500	Corona
1	0.0222	0.0214	0.0204	0.0180
2	0.0289	0.0307	0.0258	0.0216
3	0.0322	0.0254	0.0293	0.0287
4	0.0251	0.0236	0.0202	0.0207
5	0.0248	0.0236	0.0204	0.0209
6	0.0264	0.0238	0.0196	0.0206
7	0.0260	0.0258	0.0223	0.0221
8	0.0244	0.0228	0.0219	0.0219
9	0.0251	0.0250	0.0211	0.0229
10	0.0263	0.0249	0.0226	0.0221
11	0.0275	0.0268	0.0203	0.0219
12	0.0252	0.0234	0.0207	0.0228
13	0.0270	0.0270	0.0261	0.0281
14	0.0258	0.0269	0.0242	0.0247
15	0.0272	0.0275	0.0233	0.0238
16	0.0299	0.0316	0.0235	0.0246
17	0.0386	0.0390	0.0255	0.0277
18	0.0344	0.0368	0.0268	0.0284
19	0.0330	0.0348	0.0293	0.0307
20	0.0349	0.0361	0.0241	0.0299
21	0.0342	0.0362	0.0290	0.0305
22	0.0379	0.0388	0.0335	0.0352
23	0.0419	0.0422	0.0342	0.0353
24	0.0456	0.0476	0.0318	0.0320
25	0.0532	0.0552	0.0377	0.0381
26	0.0564	0.0589	0.0428	0.0432
27	0.0532	0.0556	0.0400	0.0410
28	0.0561	0.0568	0.0437	0.0449
29	0.0561	0.0568	0.0444	0.0469
30	0.0517	0.0512	0.0424	0.0526
31	0.0505	0.0503	0.0489	0.0491
32	0.0592	0.0600	0.0524	0.0529
33	0.0537	0.0547	0.0482	0.0490
34	0.0496	0.0521	0.0529	0.0549
35	0.0539	0.0550	0.0498	0.0510
36	0.0550	0.0557	0.0496	0.0497

	Core E	Core E	Core F	Core F
Slice	6500	Corona	6500	Corona
37	0.0589	0.0602	0.0510	0.0515
38	0.0554	0.0561	0.0515	0.0525
39	0.0566	0.0580	0.0519	0.0544
40	0.0484	0.0569	0.0470	0.0478
41	0.0556	0.0567	0.0580	0.0589
42	0.0589	0.0595	0.0563	0.0565
43	0.0523	0.0517	0.0613	0.0609
44	0.0567	0.0588	0.0549	0.0533
45	0.0596	0.0626	0.0604	0.0604
46	0.0495	0.0499	0.0626	0.0633
47	0.0591	0.0585	0.0520	0.0516
48	0.0583	0.0567	0.0562	0.0574
49	0.0533	0.0496	0.0499	0.0524
50	0.0425	0.0404	0.0598	0.0607
51	0.0450	0.0425	0.0556	0.0559
52	0.0414	0.0372	0.0650	0.0648
53	0.0465	0.0449	0.0516	0.0504
54	0.0466	0.0409	0.0540	0.0533
55	0.0444	0.0383	0.0455	0.0468
56	0.0449	0.0421	0.0466	0.0464
57	0.0412	0.0358	0.0539	0.0536
58	0.0466	0.0424	0.0396	0.0381
59	0.0363	0.0339	0.0422	0.0400
60	0.0437	0.0426	0.0428	0.0420
61	0.0417	0.0387	0.0422	0.0384
62	0.0363	0.0385	0.0421	0.0384
63	0.0432	0.0414	0.0438	0.0384
64	0.0426	0.0440	0.0379	0.0318
65	0.0404	0.0383	0.0448	0.0391
66	0.0493	0.0437	0.0436	0.0378
67	0.0372	0.0371	0.0406	0.0372
68	0.0429	0.0391	0.0420	0.0400
69	0.0431	0.0407	0.0386	0.0376
70	0.0459	0.0424	0.0390	0.0371
71	0.0449	0.0459	0.0403	0.0388
72	0.0445	0.0467		
73	0.0418	0.0441		
74	0.0491	0.0511		
75	0.0606	0.0620		
Total, g	3.238	3.214	2.873	2.876